Drivers of Spatiotemporal Variability of Ecosystem Metabolism in Aridland Streams

by

Mengdi Lu

A Thesis Presented in Partial Fulfillment
of the Requirements for the Degree
Master of Science

Approved December 2021 by the
Graduate Supervisory Committee:

Nancy Grimm, Co-Chair
John Sabo, Co-Chair
Christofer Bang

ARIZONA STATE UNIVERSITY

May 2022

ABSTRACT

Stream metabolism is a critical indicator of ecosystem health and connects stream ecology to global change. Hence, understanding the controls of metabolism is essential because streams integrate land use and could be net sources or sinks of carbon dioxide (and methane) to the atmosphere. Eleven aridland streams in the southwestern US (Arizona) across a hydroclimatic and size (watershed area) gradient were surveyed, and gross primary production (GPP) and ecosystem respiration (ER) were modeled and averaged seasonally over a period of 2-4 years. The seasonal averaged GPP went as low as 0.001 g $O_2m^{-2}d^{-1}$ (Ramsey Creek in 1st quarter of 2017) and as high as 14.6 g $O_2m^{-2}d^{-1}$ (Santa Cruz River in 2nd quarter of 2017), whereas that of ER ranged from 0.003 (Ramsey Creek in 1st quarter of 2017) to 20.3 g $O_2m^{-2}d^{-1}$ (Santa Cruz River in 2nd quarter of in 2017). The coefficient of variation (CV) of these GPP estimates within site ranged from 42% (Upper Verde River) to 157% (Wet Beaver Creek), with an average CV of GPP 91%, whereas the CV of ER ranged from 32% (Upper Verde River) to 247% (Ramsey Creek), with an average CV of ER 85%. Among 4 main categories of hypothetical predictors (hydrology, nutrient concentration, local environment, and size) on CV and point measurement of stream metabolism, the following conclusion was made: hydrologic variation only predicted the ER and CV of ER but not the GPP or CV of GPP; light and its CV controlled GPP and its CV, respectively, whereas temperature was one of the controlling factors for ER; CV of nutrient concentration was one of the drivers of CV of GPP, nitrate concentration was correlated with point measurement of GPP and ER while soluble reactive phosphorus (SRP) concentration was only relevant to GPP; watershed area was correlated with CV of GPP, while depth mattered to both GPP and ER. My work will enhance our understanding of streams at multiple temporal and spatial scales and ultimately will benefit river management practice.

ACKNOWLEDGMENTS

First and foremost, I am extremely grateful to my supervisors, Prof. Nancy Grimm and Prof. John Sabo for their invaluable advice, continuous support, and patience during my study. Their immense knowledge and plentiful experience have encouraged me in all the time of my academic research and daily life. I would also like to thank Dr. Tamara Harms, Dr. Bob Hall for their technical support and academic advice on my study, and Dr. Albert Ruhí, Dr. Ethan Baruch and our lab technician Leah Gaines-Sewell for their help in the field work. Besides, I would like to express my gratitude to Dr. Christofer Bang for his treasured support and being my defense committee member. I would like to thank all the members in the Sabo Lab and Grimm Lab. It is their kind help and support that have made my study and life in the US a wonderful time. Finally, I would like to express my gratitude to my parents and my friends. Without their tremendous understanding and encouragement in the past few years, it would be impossible for me to complete my study.

TABLE OF CONTENTS

Page

LIST OF TABLES v

LIST OF FIGURES vi

INTRODUCTION 1

STUDY SITE AND METHODS 4

Study Site 4

Data Collection and Metabolism Modeling 6

Characterizing Features of the Discharge Variation 9

Visualizing the Discharge Seasonality 9

Identifying Hydrologic Regimes Using Anomalies 10

Analyzing the Shift Between Different Regimes 11

Data Analysis: Drivers of Spatiotemporal Variation in Metabolism of Aridland Streams 12

RESULTS 14

Ecosystem Metabolism in Aridland Streams 14

Hydrological Features of Aridland Streams 20

Within-Year (Seasonal) Signal of Streamflow 20

Hydrologic Regimes and Regime Shifts 23

Drivers of Spatiotemporal Variation in Stream Metabolism 27

Controls on the Seasonal Mean GPP and ER 27

Controls on the Variance of Stream Metabolism 30

DISCUSSION 33

Seasonal Stream Metabolism in Aridland and the CV of Stream Metabolism 35

Features of Hydrologic Variations of Aridland Streams 36

Hydrology Predicting ER but Not GPP 38

PAR Correlated with GPP and Temperature Correlated with ER 39

Nutrient Concentrations Determining GPP and ER 40

Water Depth Driving Stream Metabolism and Watershed Area Driving CV of GPP 41

Page

CONCLUSION 42

REFERENCES 44

APPENDIX 54

A TABLES AND FIGURES 55

LIST OF TABLES

Table Page

1. Table 1: Basic Information of Study Sites and Data Collection 5
2. Table 2: Seasonal Mean GPP and ER 17
3. Table 3: Mean and CV of Seasonal Mean GPP and ER 18
4. Table 4 A: PCA Result : the First 3 Principal Components of Seasonal Mean of Water Chemistry Variables 28
5. Table 4 B: The Matrix of Seasonal Mean of Water Chemistry Variable Loading 28
6. Table 5: MLR Result Using Mean GPP and ER as Response Variables 29
7. Table 6 A: PCA Results: the First 3 Principal Components of Seasonal Mean of Water Chemistry Variables 31
8. Table 6 B: The Matrix of Chemistry Variable Loadings 31
9. Table 6 C: PCA Result: the First 3 Principal Components of Hydrological Variables 31
10. Table 6 D: The Matrix of Chemistry Variable Loadings 31
11. Table 7: LR Result Exploring the Correlation Between Size (Watershed Area) And Other Predicted Variables 32
12. Table 8: MLR Result Using CV of GPP and ER as Response Variables 32

LIST OF FIGURES

Figure Page

1. Figure 1: Map of Study Sites 5

2. Figure 2: Stream Metabolism for Each Stream Averaged by Season. A: Seasonal Mean GPP; B: Seasonal Mean ER; C: Seasonal Mean GPP: Seasonal ER Ratio (P:R) 19

3. Figure 3: Seasonal Signal of Streamflow, 11 Streams Were Categorized into 4 Subsets. A: Winter; B: Summer; C: Bimodal; D: Flashy 21

4. Figure 4 a, b, c, and d: DFFT Result- Annual Extreme Residuals of Discharge Along Time. a: Winter; b: Summer; c: Bimodal; d: Flashy 25

4. Figure 4 A, B, C and D: DFFT Result- Net Annual Anomalies and Delta Net Annual Anomalies of Each Year. A: Winter; B: Summer; C: Bimodal; D: Flashy 25

5. Figure 5: Scale-average Time Series of Max Annual Aggregate Blue Noise Power Along Time 26

INTRODUCTION

Ecosystem metabolism (photosynthesis and respiration) is a fundamental property of ecosystems. In streams, gross primary productivity (GPP) represents the amount of organic matter synthesized by photosynthetic organisms or autotrophs; ecosystem respiration (ER) results from the breakdown of organic matter by both autotrophs and heterotrophs (Webster et al. 1995; Mulholland et al. 2001). Together they demonstrate energy flow through food webs (Bernhardt et al. 2017), and are important indicators of biogeochemical cycling, especially nutrient cycling driven by carbon cycling (Cole et al. 2007; Tranvik et al. 2009). Stream metabolism provides an integrative quantification of nutrient dynamics and energy supply and dissipation (Izagirre et al. 2008; Williamson et al. 2008). Understanding stream metabolism can help us further quantify ecosystem services (Hall and Tank, 2003; Sobota et al. 2012), like pollution abatement and nutrient retention (Gücker and Pusch, 2006; Merseburger et al. 2011); and quantify ecosystem function, such as the fate of terrestrial carbon fixation, allochthonous subsidies to aquatic food webs, and food-web energy fluxes (Tranvik et al. 2009; Cole et al. 2011).

Stream metabolism varies in space across river basins and networks (e.g., Finlay 2011; Yates et al. 2013; Dodds et al. 2018) and in time from season to season and from year to year (e.g., Uehlinger and Naegeli, 1998; Roberts et al. 2007; Beaulieu et al. 2013), which reflects differences in the abiotic environment across similar spatial and temporal scales (Roberts et al. 2007; Yates et al. 2013). Much of our understanding of factors controlling stream metabolism derives from work

on single streams in different biomes or climate zones (Marzolf et al. 1994; Mulholland, 2001), or streams affected by land-use change (Young and Huryn, 1999; Guecker et al. 2009). Many factors affect the rates of GPP and ER, including light availability (Dodds et al. 1999; Mulholland et al. 2001; Roberts et al. 2007, Bernhardt et al. 2018), riparian canopy (Uehlinger, 2006), nutrient concentration (Grimm and Fisher, 1986; Guasch et al. 1995) and hydrologic conditions (Acuna 2004; Acuna et al. 2004; Roberts et al. 2007). However, researchers have seldom compared spatial variation in the temporal variability in GPP and ER of streams in response to spatial variation in temporal variability of key drivers like hydrology, nutrient concentrations, temperature and light (Cole et al. 1991, Hall 2016). Further, few studies have assessed how these factors may interact with each other to influence stream metabolism and how these factors vary in relative importance across streams (but see Mulholland et al. 2001; Bernot et al. 2010; Savoy et al. 2019, Koenig et al. 2019). Hence, there is a need for a more detailed description of the spatiotemporal patterns of metabolism in streams. Here, I use a hydroclimatic gradient to examine the role that hydrologic regime, nutrient concentration, and environmental factors including geomorphology play directly and indirectly in the spatial and temporal variation in GPP and ER.

In arid and semiarid regions, many once-perennial rivers are becoming intermittent due to water appropriation (Sabo et al. 2010; Sabo et al. 2017) and climatic drying (Larned et al. 2010; Gleick 2003). Despite the temporary appearance of non-perennial streams and rivers on the landscape, they are critical to the health of river systems and networks, providing essential functions and values just as larger perennial rivers (Meyer et al. 2003; Nadeau and Rains, 2007; Larned et al.

2010). In the US Southwest, most desert streams and rivers are intermittent, and they experience cycles of flooding and drying (Lake, 2003) and extremes in streamflow (Moran et al. 2019) that make them ideal systems to study space-time variability of physical characteristics. These aridland streams and rivers share some similarities in hydrologic regimes and physical environment at local and regional or watershed scales, and hence, in the resulting ecological processes. For instance, relatively high temperature and abundant light in the warm desert regions of Arizona favor high in-stream productivity that may at times exceed ecosystem respiration (Minshall 1978; Grimm 1987; Lamberti and Steinman 1997; Sinsabaugh 1997, Uehlinger et al. 2002). Illustrating the spatial difference in seasonal GPP and ER and their variance in aridland streams and quantifying the drivers and constraints on stream metabolism is difficult (Bernhardt et al. 2018). Seasonal and interannual patterns reflect a highly dimensional and multiscale set of morphological, biogeochemical, and hydrologic controls that challenge comparisons across streams (Savoy et al. 2019), given the extremely dynamic nature of aridland streams. Failure to understand how and why stream metabolism differs in space and time will limit our potential to monitor alterations to non-perennial stream networks that result from climate change and development activities (Hamada 2016). Here, I contribute to filling that knowledge gap by relating rates and variance in stream metabolism across four years to differences among 11 aridland streams in hydroclimatic regime and other environmental variables.

In this research, multiple short-term (mostly <7 days) measurements of GPP and ER were averaged to represent seasonal stream metabolism, streams were categorized in accordance with

features of their seasonal flow signals, and interannual and seasonal discharge variations were characterized. I addressed how differences in size represented by the watershed area, local environment (water temperature and photosynthetically active radiation), nutrient concentrations, and hydrological variability impacted stream ecosystem metabolism. Additionally, I focused on how the variance of these potentially influential variables controlled the variance of GPP and ER.

STUDY SITE AND METHODS

Study site

Chosen sites were 11 first- to third-order, gauged streams in Arizona draining hot desert to semi-arid mountainous watersheds (Table 1, Figure 1). The streams were located across a hydroclimatic gradient from dominance by strong Pacific winter precipitation driven by frontal storms and weak summer monsoonal precipitation to dominance by strong monsoonal precipitation with weak winter frontal rainfall. The similarities and dissimilarities in overall climate facilitated comparisons across the hydroclimatic gradient of seasonal and interannual variation in biological patterns and processes, as well as further exploration of the complicated interactions among hydrology, meteorology, and geomorphology and response of stream systems. Each year is divided into 4 quarters, as the 1st quarter starts in January and ends in March, the 2nd and 3rd quarters comprise April, May, June, and July, August, September, respectively. The 4th quarter includes October, November, and December. The summer monsoon usually occurs during the 3rd quarter whereas the winter frontal storms are often seen during the 1st quarter.

Table 1: Basic information of study sites and data collection. Site number corresponds to numbers on the Map (Figure 1).

Stream and Number on the Map	Watershed area (km^2)	USUS station ID	Historic discharge data length (years, to 2020)	Metabolism data
Agua Fria River (AF, #1)	1498	9512500	80	2016-2019
Babacomari River (BB, #2)	409	9471380	19	2016-2017
Bonita Creek (BN, #3)	773	9447800	39	2016-2019
Eagle Creek (EG, #4)	1592	9447000	76	2016-2019
Ramsey Creek (RM, #5)	20	9470750	20	2016-2017
San Francisco River (SF, #6)	4273	9444500	96	2016-2017
San Pedro River (SP, #7)	3159	9471000	116	2016-2019
Santa Cruz River (SC, #8)	210	9480500	71	2016-2019
Sycamore Creek (SY, #9)	420	9510200	60	2016-2017
Upper Verde River (VD, #10)	5504	9503700	59	2016-2017
Wet Beaver River (WB, #11)	284	9505200	59	2016-2017

Figure 1: Map of study sites. Site number corresponds to numbers in Table 1.

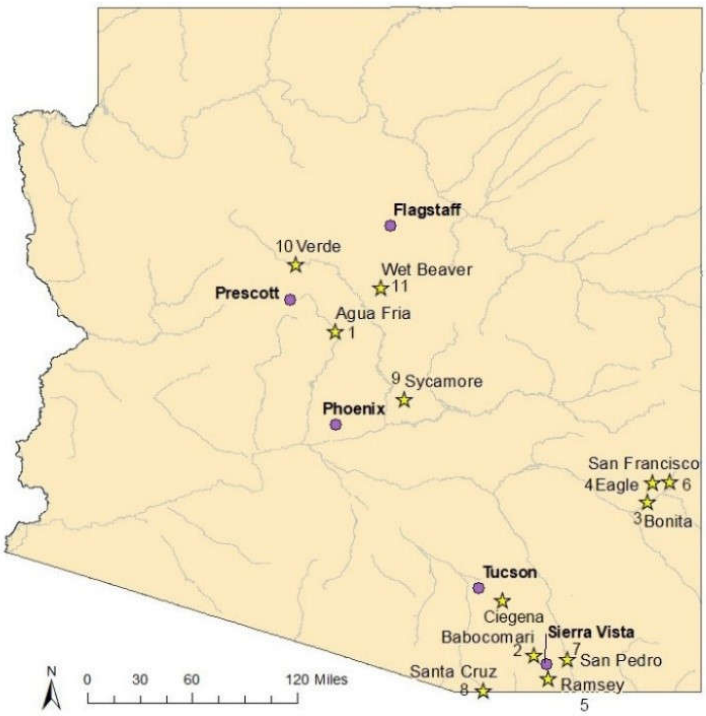

Data collection and metabolism modeling

Estimation of stream metabolism, i.e., daily GPP and ER, was based on the single-station diel dissolved oxygen (DO) change method (Odum 1956), implemented by applying measured changes in DO over several-day periods using the R package streamMetabolizer (https://github.com/USGS-R/streamMetabolizer). Specifically, daily variation in oxygen production and consumption by stream organisms was used to estimate GPP and ER:

$$dDO/dt = (GPP+ER)/z + K(DO_{sat}-DO)$$

dDO/dt is the change in dissolved oxygen concentration through time.

GPP is the rate of production of photosynthetic O_2, in units of oxygen, g $O_2 m^{-2} d^{-1}$

ER is the rate of consumption of oxygen through autotrophic and heterotrophic respiration, in units of oxygen, g $O_2 m^{-2} d^{-1}$

K is gas exchange rate coefficient, governing the volume of net oxygen exchange between the water column and the overlying air

$K(DO_{sat}-DO)$ is the volume of net oxygen exchange

In the field, sensors were deployed at the upstream and downstream boundaries of each study reach, collecting time series data of dissolved oxygen (DO), water temperature, air pressure, and conductivity at 10-min intervals (YSI sensors; Yellow Springs, OH), and photosynthetically active radiation (PAR) at 5-min intervals (Odyssey sensors; mfr info). For each stream during each survey, two different modeling scenarios using observed (Obs_light) and modeled light values (Mod_light)

were set up for both upstream (UP) and downstream (DOWN) locations. The ‘Obs_light’ model averages data collected from upstream and downstream Odyssey sensors to better reflect the energy received by the stream reach during observation, whereas for the the ‘Mod_light’ scenario, an estimate of solar insolation was made using the light model in the streamMetabolizer package based on the geographic location, elevation, date, and daily maximum PAR. Three cross sections at the upstream, downstream, and midpoint of the 100-m study reach were chosen by the field team to measure multiple water depth at 30-cm intervals of each cross section. The median of these measurements was used to represent the water depth over the sampling periods (<3 days), whereas during longer surveys (>3 days), linear interpolation between two median depths was applied to reflect changes in morphometry throughout the survey (i.e., as the stream dried or flooded). A linear regression between point measurement of discharge at each site and discharge data taken from the corresponding nearest USGS gauge station at the same time was used to calibrate the continuous discharge data and better represent the real discharge condition of study reaches. Daily GPP and ER at upstream (UP) and downstream (DOWN) locations of each study reach were modelled separately based on the YSI sensor data, light data (Mod_light and Obs_light modeling scenarios), water depth, and calibrated discharge.

Initially the nighttime regression model in the streamMetabolizer package was applied to estimate the gas exchange coefficient, K600, and the output was compared with on-site measurement to better set priors (daily bin positions to pool K600 values) for hierarchical Bayesian model. This state-space model is hierarchically structured and includes both observation and process error,

allowing us to use information from many days to inform estimates on each individual day (Appling et al. 2018). I accepted the default model specifications including the initial daily mean and standard deviation of GPP and ER. The model was fit with Markov Chain Monte Carlo (MCMC) sampler in Stan (Carpenter et al. 2017). The estimation was made with 18,000 MCMC samples from the posterior distribution after parameters were converged. The Gelman-Rubin convergence statistic (R-hat $\hat{R}$ statistic) of the MCMC sampling for each MCMC iteration was checked and all R-hat values of GPP, ER, K600 and process error were below 1.1, indicating the convergence of the three MCMC chains used in the model. R^2 between measured DO and modeled DO was calculated to evaluate fitting of the two model scenarios using modeled light and observed light, and the result with higher R^2 was retained. Finally, estimates from upstream and downstream locations were averaged after poor-fitting results ($R^2 < 0.4$) were dropped. GPP and ER were both expressed in units of mass oxygen per unit area per time, g $O_2 m^{-2} d^{-1}$, and daily net ecosystem productivity (NEP, g $O_2 m^{-2} d^{-1}$) was calculated as the balance of daily GPP and ER values.

Additionally, water samples were collected during each survey, and standard methods were applied during samplings, sample preparations and analytics (American Public Health Association and American Water Works Association, 1995). Ammonium and soluble reactive phosphorus (SRP) were analyzed by colorimetry using an automated discrete analyzer. Chloride, fluoride, nitrate and sulphate were measured by ion chromatography. Total nitrogen and dissolved organic matter were determined by chemical oxidation. Sodium and potassium were analyzed using a flame analyzer while calcium and magnesium were analyzed by atomic absorption spectrometer.

Characterizing features of the discharge variation

To give historical reference for observations collected in specific years, I quantified the seasonal and stochastic components of streamflow variation for each site using long-term data preceding the metabolism measurements (see Table 1 for discharge data length).

Visualizing the discharge seasonality

Long-term discharge data were imported from USGS website using R package waterData and log transformed. Plots were generated based on log-normalized discharge against the ordinal days (day 1 to day 365) for each of the study site with the seasonal discharge signal overlaid. The signal was specified as non-stationary and simple linear regression was applied to estimate the long-term linear trend. The residuals were used to calculate the seasonal signal. Predicted flow and corresponding residual at each time point were calculated from seasonal signal and long-term trend coefficient. By visualization these streams were categorized into 4 different subsets in accordance with the timing of the streamflow signal within year. Winter rain-dominated streams always have peak discharge before day 100 (hereafter “winter” category), and summer monsoon-dominated streams usually experience only one sharp increase in discharge in summer after day 200 (hereafter “summer” category). If two peaks were captured, the streams were impacted by the mixed effect of both winter frontal and summer monsoon (referred as “bimodal” category). Streams with no significant peaks detected throughout the year were labeled as “flashy” representing either “flashy” or “constant” sites (referred as “flashy” category).

Identifying hydrologic regimes using anomalies

Discrete Fast Fourier Transform (DFFT) applied to the normalized, log10-transformed mean daily streamflow data allowed for decomposition of the time-series data and extraction of featured frequencies and amplitudes to reconstruct the long-term seasonal signal in periodic flow variation (Sabo and Post, 2008). DFFT can also identify daily anomalies referenced to the seasonal patterns. The time series of daily average discharge anomalies was given by the difference between observed and expected daily variation, and the whole record was computed to extract three strings of yearly anomalies: high-flow anomalies (the maximum yearly high-flow anomaly), low-flow anomalies (the minimum yearly low-flow anomaly), and net annual anomalies (NAA, the yearly sum of all daily residuals). High- and low-flow anomalies represent the severity or magnitude of the most extreme events of each year, whereas net annual anomalies enable easy comparison of the observed year with respect to the historic record; years with positive NAA are 'wetter' years than the long-term record, or high-flow-dominated years (hereafter "wet" regime), whereas negative NAA means low-flow-dominated, or 'drier' (hereafter "dry" regime). These three annual indices were calculated for each stream to collectively quantify the distance and direction to which the hydrologic regime in a particular year deviated from historic seasonal expectations. Delta NAA was also calculated as the difference between the NAA of the current year and the previous year to show the yearly variation in the interannual net anomalies. For comparison purpose, only the most recent 20 years discharge data were taken, and annual extreme residuals were detected using R package discharge (Shah et al. 2019). Catastrophic variability for high and low flow events was also explored

with the help of this R package and the following parameters were calculated for each stream: flood pulse extent (FPext), high spectral anomaly frequency (HSAF), low spectral anomaly frequency (LSAF), high spectral anomaly magnitude (HSAM), low spectral anomaly magnitude (LSAM), mean Net Annual Anomaly (NAA), catastrophic variability for high and low flow events (HFsigma and LFsigma respectively), and signal noise ratio (snr) (Sabo et al. 2017).

Analyzing the shift between different regimes

Regime shift can be illustrated visually by abrupt transitions between strings of positive and negative anomalies. The structure of the variances in the anomalies was explored using a spectral method, wavelet analysis, which decomposes nonstationary time series into scale- and location-specific measures of frequency-power (Cazelles et al. 2008; Torrence and Compo, 1998). The hydroclimate of the study systems is influenced by overlapping ENSO and PDO cycles and the seasonal discharge signals experience change in frequency over time (Sabo and Post, 2008). Wavelets sheds lights on the transit times of regime shifts between strings of high- and low-flow years by quantifying the time scales (e.g., in years) and locations (dates in the time series within bands of frequency, i.e., El Niño, 3-5 years, or Decadal Oscillations, 10 years) of regime shifts (Foufoula-Georgiou and Kumar, 1994). Specifically, Morlet mother wavelet function was applied on the daily discharge anomalies against a theoretical blue-noise background using the discharge (Shah et al. 2019) and WAVELETCOMP (Roesch and Schmidbauer, 2014) packages in R. Significant blue noise in the wavelet scalogram represents negative autocorrelation (i.e., regime

shift), and was identified across multiple time scales (1-2 years). A time series of annual power maxima was calculated, reflecting peak transition periods between wet and dry regimes. Maximum shift between regimes is illustrated by time series of peak transition (maximum annual significant blue noise). Significant peak transition was detected based on 95% confidence interval (CI) of normal distribution. The features of regime shift, including the lag time since last peak (RT_{recent}), the relative consistency of return interval (i.e., coefficient of variation of return interval) (CV_{RT}) etc. were calculated.

Data analysis: drivers of spatiotemporal variation in metabolism of aridland streams

Local environmental drivers of the variation of the seasonal mean of GPP and ER for each site during each survey were studied, along with the factors that contributed to the spatial difference in the coefficient of variation (CV) of the seasonal GPP and ER. Two **Principal Component Analyses (PCA)** were run first to summarize the information content and reduce the dimensionality in this high-dimension database, as multiple predicted factors that might contribute to the CV of seasonal GPP and ER from site to site were proposed. Due to the small sample size (11 streams), I sought a smaller set of summary indices that could be more easily visualized and analyzed. The first PCA was applied on the CV of all the available concentration data of SRP, DOC, fluoride, chloride, sulfate, nitrate, sodium, ammonium, potassium, magnesium and calcium. Another PCA was run on the hydrologic variables, including maximum annual aggregate blue noise power, flood pulse extent (FPext), high spectral anomaly frequency (HSAF), low spectral anomaly frequency

(LSAF), high spectral anomaly magnitude (HSAM), low spectral anomaly magnitude (LSAM), mean Net Annual Anomaly (NAA), catastrophic variability for high and low flow events (HFsigma and LFsigma respectively), and signal noise ratio (snr). The model with variables explaining over a certain percentage of the total variability was kept for subsequent analyses and only the first principal component (PC1) in each of the PCA was saved. **Multiple linear regression (MLR)** techniques were then employed as an exploratory tool targeting potential drivers controlling the CV of GPP and ER. Linear mixed-effect analysis was conducted with the R package of nlme (Zuur et al. 2009), with CV of GPP and ER as the response variables. PC1 of the water chemistry parameters and PC1 of the hydrological variables, the CV of water temperature and CV of? PAR were treated as the explanatory variables. The 'lme4' package in R was used to fit the linear mixed effect models, as these variables are considered to be independent across site but correlated within site. The constant variance function structure using varIdent, which allows different variances according to level of categorical factors (site and season), was used instead of the unstructured variance function structure when the former had lower Akaike Information Criterion (AIC) values, indicating better model fits. Analysis assumptions were checked with diagnostic plots and marginal R^2 ($R^2_{MLR(m)}$) for fixed effects, and conditional R^2 ($R^2_{MLR(c)}$) for both fixed and random effects was calculated using the MuMIn package.

Analytical models were also set up to determine the drivers of seasonal mean GPP and ER. PCA was conducted on the same set of water chemistry parameters, including soluble reactive phosphorus (SRP), DOC, fluoride, chloride, sulfate, nitrate, sodium, ammonium, potassium,

magnesium and calcium, and the first two principal components (PC1 and PC2) were used as explanatory variables in the next step, multiple linear regression analysis. The net seasonal anomaly (nsa) and seasonal sum of aggregate blue noise power (sumpower.seasonal), which were used to represent the hydrologic parameters, as well as water depth of the channel, water temperature, and PAR were all tested as explanatory variables in the MLR to explore their associations with the mean seasonal averaged GPP and ER (the response variables). Furthermore, a few individual nutrient concentration variables, PAR, water temperature, depth and one of hydrologic parameters were examined in the MLR to detect strong associations between specific nutrient concentration parameter and stream metabolism.

RESULTS

Ecosystem metabolism in aridland streams

In my study of 11 desert and mountain streams and rivers located in the arid southwestern US, the mean rate of seasonal GPP and ER across all sites was 1 g $O_2m^{-2}d^{-1}$ (ranging from 0.02 to 7 g $O_2m^{-2}d^{-1}$) and 3 g $O_2m^{-2}d^{-1}$ (ranging from 0.07 to 8 g $O_2m^{-2}d^{-1}$), respectively (Table 2). The Verde River was one of the most productive streams, with the highest GPP and ER, and Ramsey Creek had the lowest GPP and ER (Figure 2 A and B). The mean rates of metabolism across multiple sampling days within each survey varied considerably among sites and among seasons. The GPP went as low as 0.001 g $O_2m^{-2}d^{-1}$ (Ramsey Creek in 1st quarter 2017) and as high as 15 g $O_2m^{-2}d^{-1}$

(Santa Cruz River in 2nd quarter 2017), whereas ER ranged from 0.003 (Ramsey Creek in 1st quarter 2017) to 20 g $O_2m^{-2}d^{-1}$ (Santa Cruz River in 2nd quarter 2017). The temporal variation in GPP and ER were close; the CV of GPP of each site ranged from 42% (Upper Verde River) to 157% (Wet Beaver Creek), with an average CV of GPP 91%, whereas the CV of ER ranged from 32% (Upper Verde River) to 247% (Ramsey Creek), with an average CV of ER 85% (Table 3). Among all the sites, the Verde River had a substantially lower variation in both GPP and ER, whereas the highest variation of GPP from season to season occurred in Wet Beaver Creek and largest difference of ER appeared in Ramsey Creek. The 2nd quarter, comprising April, May, and June in my study and representing the pre-monsoon period, was the most productive season, with mean GPP and ER across all sites being 3 and 5 g $O_2m^{-2}d^{-1}$, respectively. On the contrary, the 4th quarter (October, November, and December) was the least productive season with the lowest average GPP of 1 g $O_2m^{-2}d^{-1}$, but this season showed the highest variance of GPP across sites (CV 147%). The lowest variance of both GPP and ER from site to site and lowest mean ER all occurred in the 1st quarter (January, February, and March), a relatively cold season associated with winter frontal storms.

On average, all streams were heterotrophic with a negative mean NEP and P:R ratios < 1 (Figure 2 C). The biggest difference between GPP and ER was seen in Agua Fria River (NEP -3 g $O_2m^{-2}d^{-1}$). More specifically, most sites had negative NEP during most surveys, with a few exceptions, such as the San Francisco River, San Pedro River, and Ramsey Creek. Autotrophic ecosystem metabolism occurred primarily in the pre-monsoon 2nd quarter; GPP was higher than ER in only 14

of 95 measurements (15%), including seven 1st-quarter surveys, three 2nd-quarter and 4th-quarter surveys respectively, and only one 3rd-quarter (monsoon) survey. Streams were close to metabolic balance in about half of the measurements, and 29 of 81 (36%) measurements were strongly heterotrophic, with P to R ratios <0.25.

Table 2: Seasonal mean GPP and ER, unit g O_2/m^2/day.

site	Season/ quarter	2016			2017			2018			2019		
		GPP	ER	NEP	GPP	ER	NEP	GPP	ER	NEP	GPP	ER	NEP
AF	1st	1.619	-3.503	-1.884				0.809	-3.654	-2.845	0.913	-0.641	0.272
	2nd	0.335	-2.429	-2.094	3.169	-8.841	-5.672	1.621	-4.636	-3.015			
	3rd	0.526	-7.603	-7.077	1.045	-2.716	-1.671	0.878	-3.352	-2.475			
	4th	0.085	-3.804	-3.719	0.746	-6.530	-5.784						
BB	1st	1.027	-2.972	-1.946	3.565	-4.769	-1.204						
	2nd	1.409	-3.396	-1.987	3.569	-5.814	-2.245						
	3rd				1.454	-5.220	-3.766						
	4th	0.319	-0.332	-0.012	2.153	-7.837	-5.685						
BN	1st	0.513	-2.955	-2.442	0.808	-3.066	-2.258	0.588	-3.350	-2.762			
	2nd	0.864	-3.582	-2.717	3.637	-8.088	-4.451	1.090	-3.430	-2.340	1.874	-3.448	-1.574
	3rd	0.821	-4.913	-4.092	1.946	-3.956	-2.010	0.402	-4.105	-3.704			
	4th	0.139	-5.056	-4.917	0.184	-3.094	-2.910						
EG	1st				0.335	-3.289	-2.954						
	2nd	0.093	-0.952	-0.859	0.205	-3.640	-3.435	1.034	-4.206	-3.172			
	3rd	0.052	-1.835	-1.783	0.209	-1.262	-1.053	0.212	-0.737	-0.525	0.644	-1.711	-1.067
	4th	0.016	-2.423	-2.407	0.063	-1.795	-1.732	0.282	-2.419	-2.137			
RM	1st	0.001	-0.004	-0.003	0.001	-0.003	-0.002						
	2nd	0.087	-0.004	0.083	0.032	-0.436	-0.404						
	3rd				0.009	-0.005	0.003						
	4th	0.005	-0.005	-0.001	0.049	-0.005	0.044						
SC	1st	1.791	-2.469	-0.678	5.102	-6.951	-1.848	0.117	-2.033	-1.915	7.180	-6.423	0.757
	2nd	4.075	-5.610	-1.535	14.593	-20.345	-5.752	0.943	-1.845	-0.902			
	3rd	1.118	-5.024	-3.906				0.367	-0.432	-0.065			
	4th	0.072	-0.276	-0.205	3.963	-5.297	-1.334						
SF	1st	0.363	-1.639	-1.276	3.271	-0.292	2.979						
	2nd	1.658	-0.880	0.778	0.619	-3.688	-3.069						
	3rd	0.635	-0.774	-0.139	1.515	-1.839	-0.323						
	4th	0.792	-0.880	-0.088	0.553	-0.258	0.295						
SP	1st	1.723	-1.555	0.168	1.918	-2.044	-0.126	2.357	-2.271	0.087	1.343	-1.722	-0.378
	2nd	1.018	-1.109	-0.091	1.715	-2.797	-1.082	3.940	-5.985	-2.045			
	3rd	1.143	-1.922	-0.779				1.444	-1.852	-0.409			
	4th	1.845	-1.775	0.070	0.764	-1.222	-0.459						
SY	1st	0.427	-2.835	-2.409	0.242	-0.241	0.001						
	2nd				1.225	-2.748	-1.523						
VD	1st	8.426	-7.414	1.011	2.266	-2.900	-0.634						
	2nd	8.380	-8.852	-0.471	10.540	-10.194	0.346						
	3rd	7.179	-10.815	-3.636	6.759	-8.352	-1.593						
	4th	5.176	-7.654	-2.478	3.572	-5.822	-2.250						
WB	1st	0.275	-1.160	-0.885									
	2nd				5.391	-10.223	-4.831						
	3rd	0.773	-1.908	-1.135	0.655	-1.867	-1.212						
	4th	0.393	-1.415	-1.021	0.229	-0.881	-0.652						

Table 3: Mean and CV of seasonal mean GPP and ER

site	GPP_mean_mean (g O_2/m^2/day)	ER_mean_mean (g O_2/m^2/day)	NEP_mean (g O_2/m^2/day)	GPP_mean_CV (%)	ER_mean_CV (%)
AF	1.068	-4.337	-3.269	79	-56
BB	1.928	-4.334	-1.860	65	-55
BN	1.072	-4.087	-3.015	92	-35
EG	0.286	-2.206	-1.920	106	-51
RM	0.026	-0.066	-0.040	124	-247
SC	3.575	-5.155	-1.580	121	-108
SF	1.176	-1.281	-0.106	82	-88
SP	1.746	-2.205	-0.459	49	-61
SY	0.631	-1.941	-1.310	83	-76
VD	6.537	-7.750	-1.213	42	-32
WB	1.286	-2.909	-1.623	157	-124

Figure 2: Stream metabolism for each stream averaged by season. A: Seasonal mean GPP (g O_2/m^2/day); B: Seasonal mean ER (g O_2/m^2/day); C: seasonal mean GPP: seasonal ER (P:R)

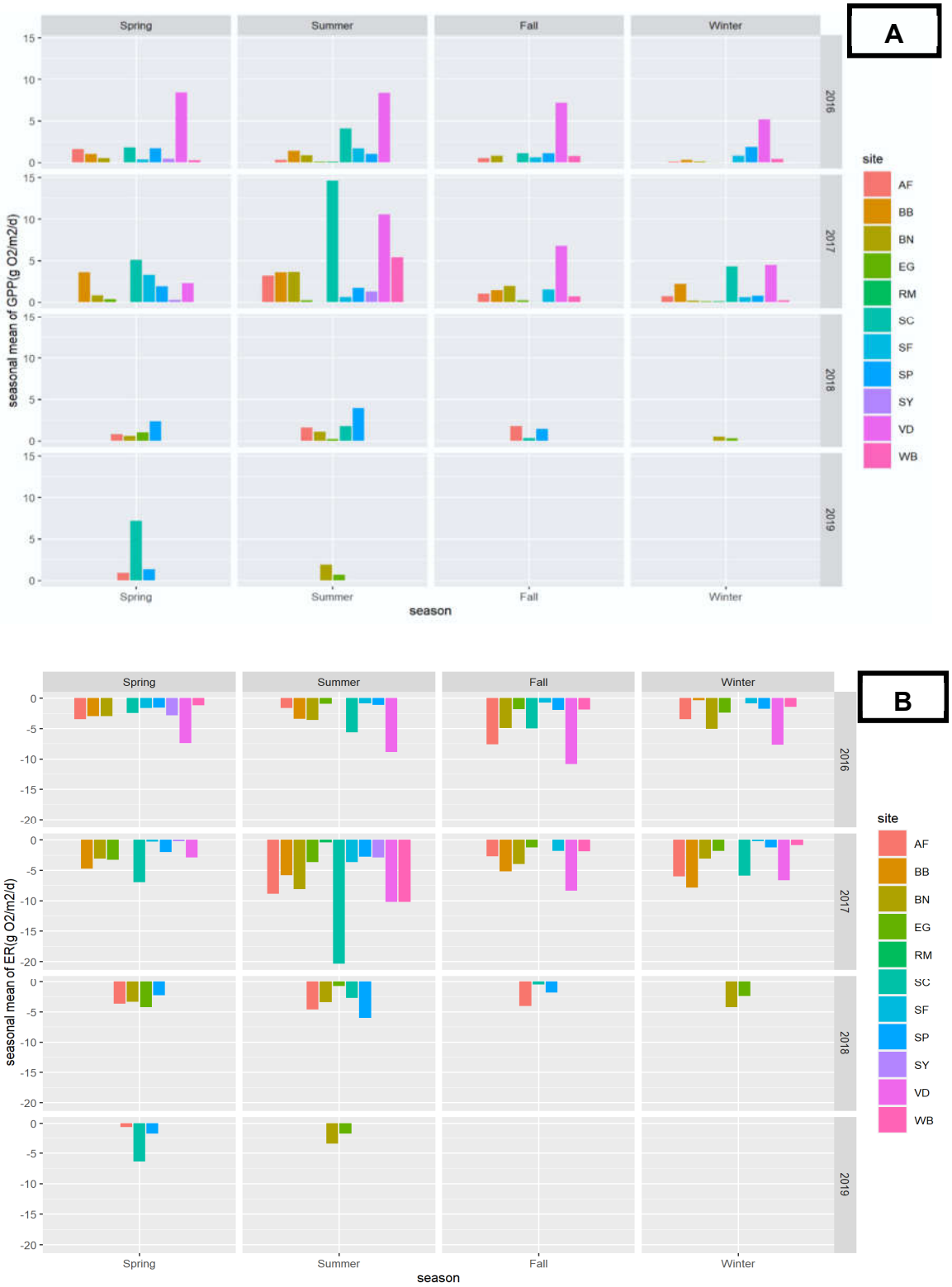

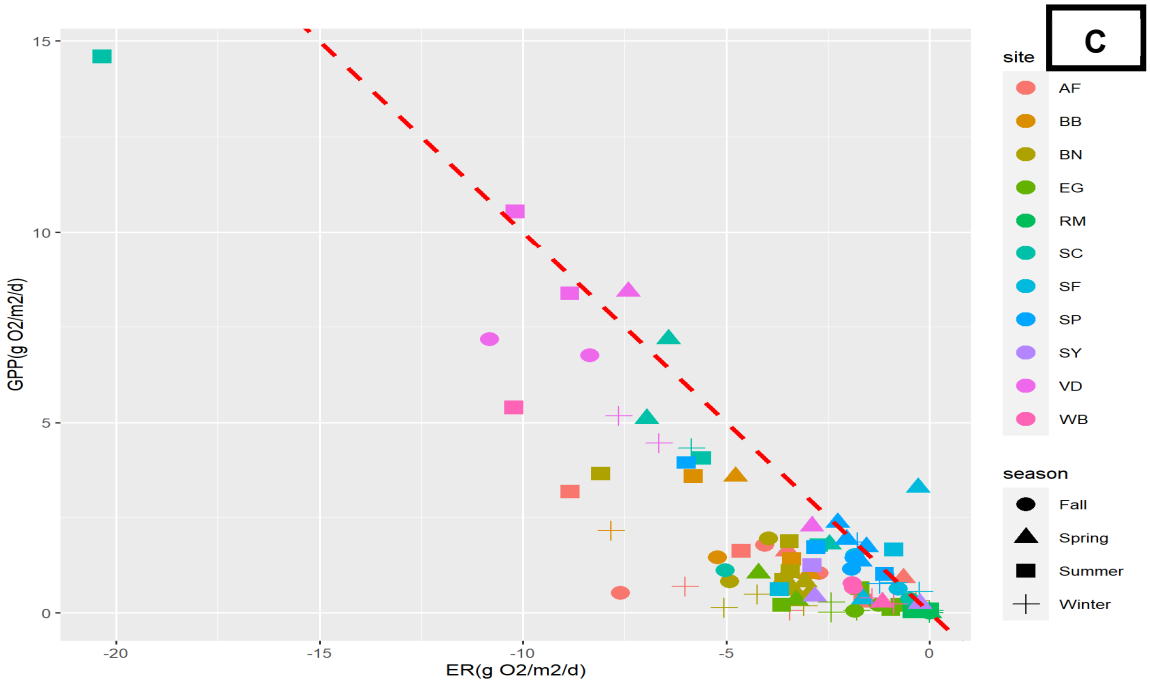

Hydrological features of aridland streams

Within-year (seasonal) signal of streamflow

The 11 study streams were categorized into four different subsets in accordance with the timing of the streamflow signal within year (Figure 3). Winter rain-dominated streams (Sycamore Creek and Wet Beaver Creek) have peak discharge before day 100 (hereafter “winter” category), and summer monsoon-dominated streams (Santa Cruz River and San Pedro River) usually experience only one sharp increase in discharge in late summer, after day 200 (hereafter “monsoon” category). If two peaks were captured, the streams were impacted by the mixed effect of both winter frontal and summer monsoon; for instance, Agua Fria River, San Francisco River, Eagle Creek and Ramsey Creek (referred to as “bimodal”). There were three other streams for which no significant peaks were detected throughout the year: Babacomari River, Bonita Creek and Verde River, so they are

labeled as “flashy” sites. Some of these streams exhibited strong seasonality in discharge. For example, the Santa Cruz and San Pedro Rivers experienced the within-year dry season and wet season repeatedly. On the contrary, no seasonality was identified in Babacomari River and Verde River. Compared with others in the “bimodal” category, the seasonality of hydrologic regime in Ramsey Creek was relatively weak.

Figure 3: Seasonal signal of streamflow, 11 streams were categorized into 4 subsets. A: Winter; B: Summer; C: Bimodal; D: Flashy.

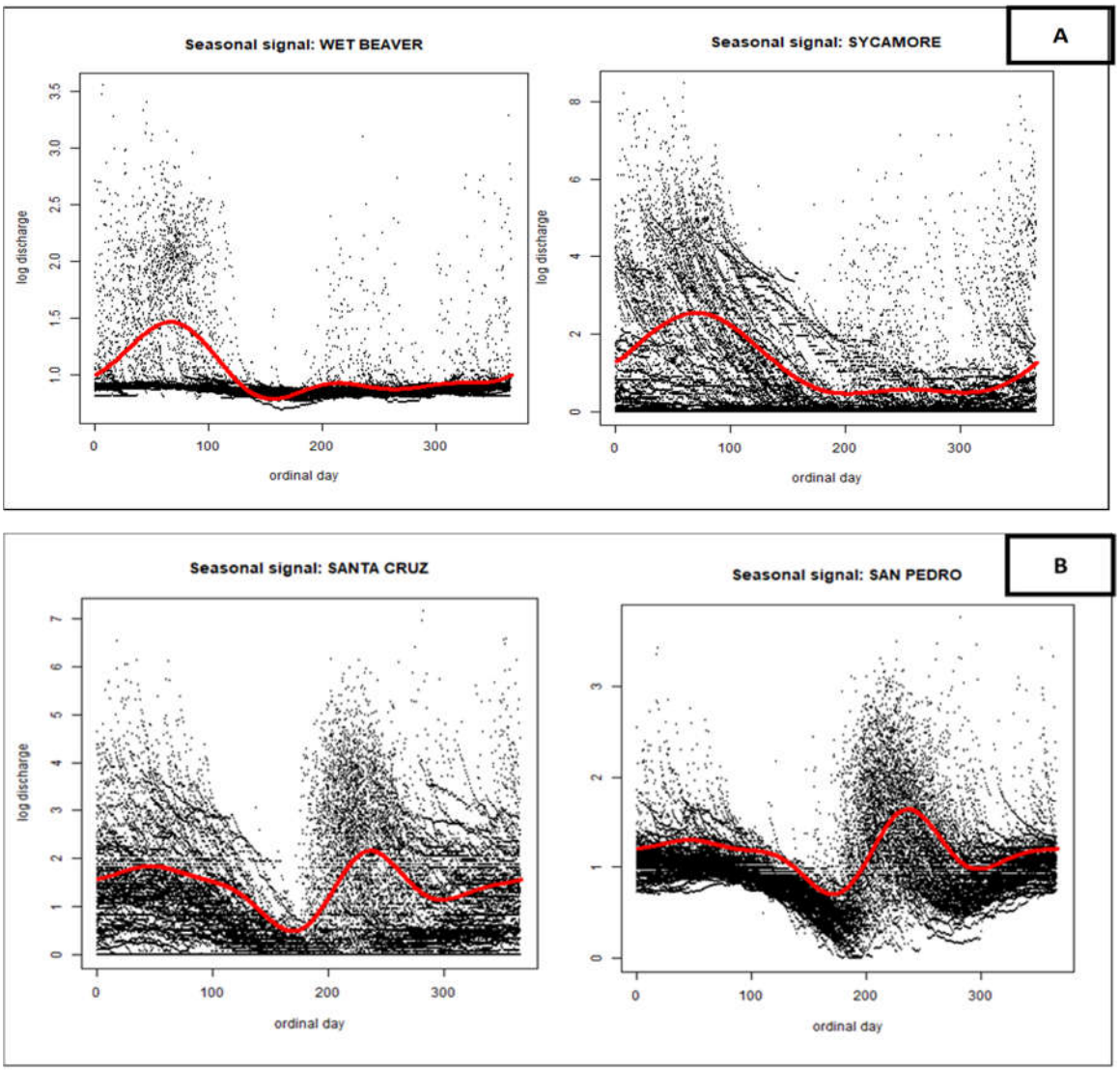

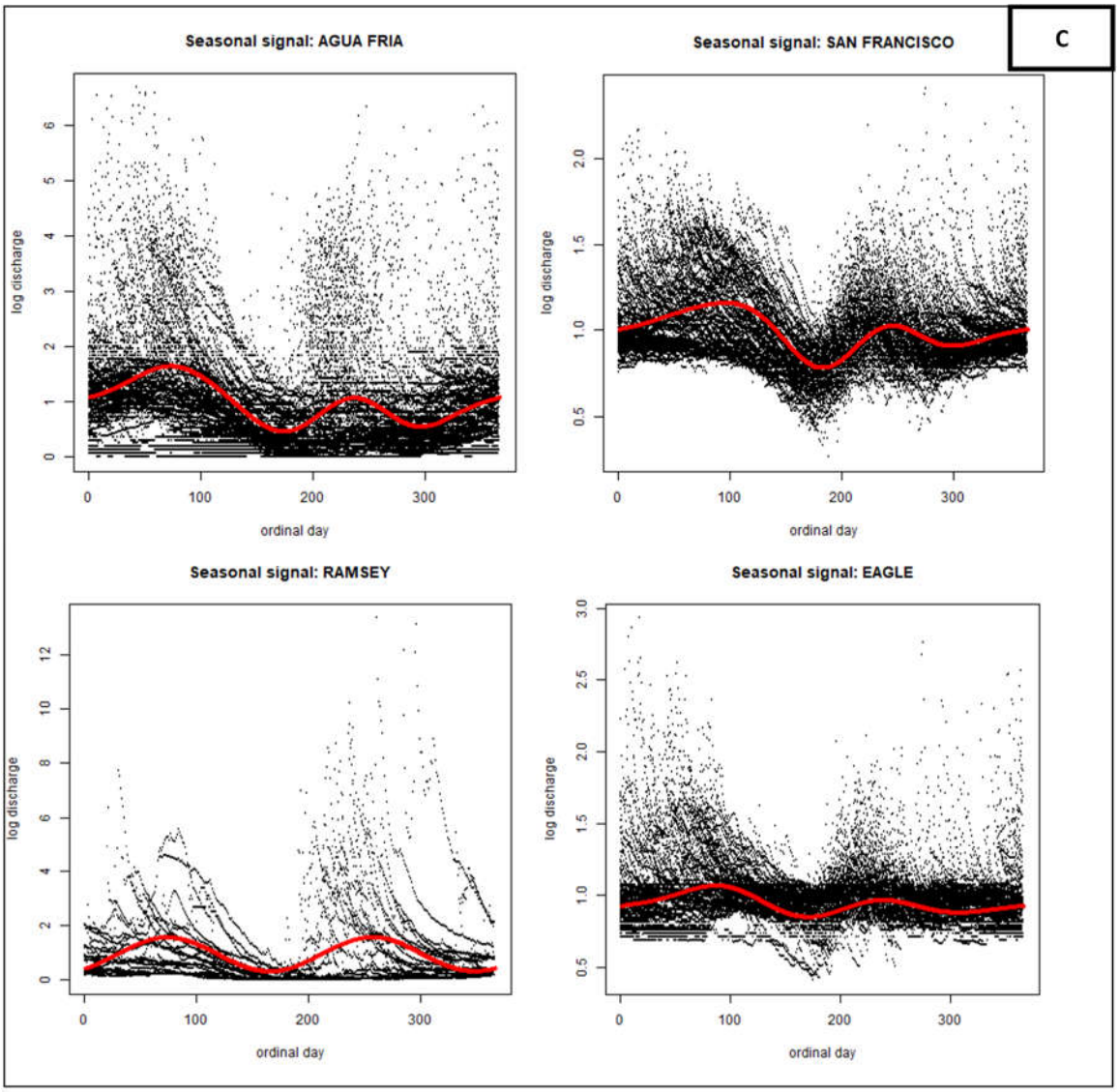
C
Seasonal signal: AGUA FRIA
Seasonal signal: SAN FRANCISCO
Seasonal signal: RAMSEY
Seasonal signal: EAGLE
log discharge
ordinal day

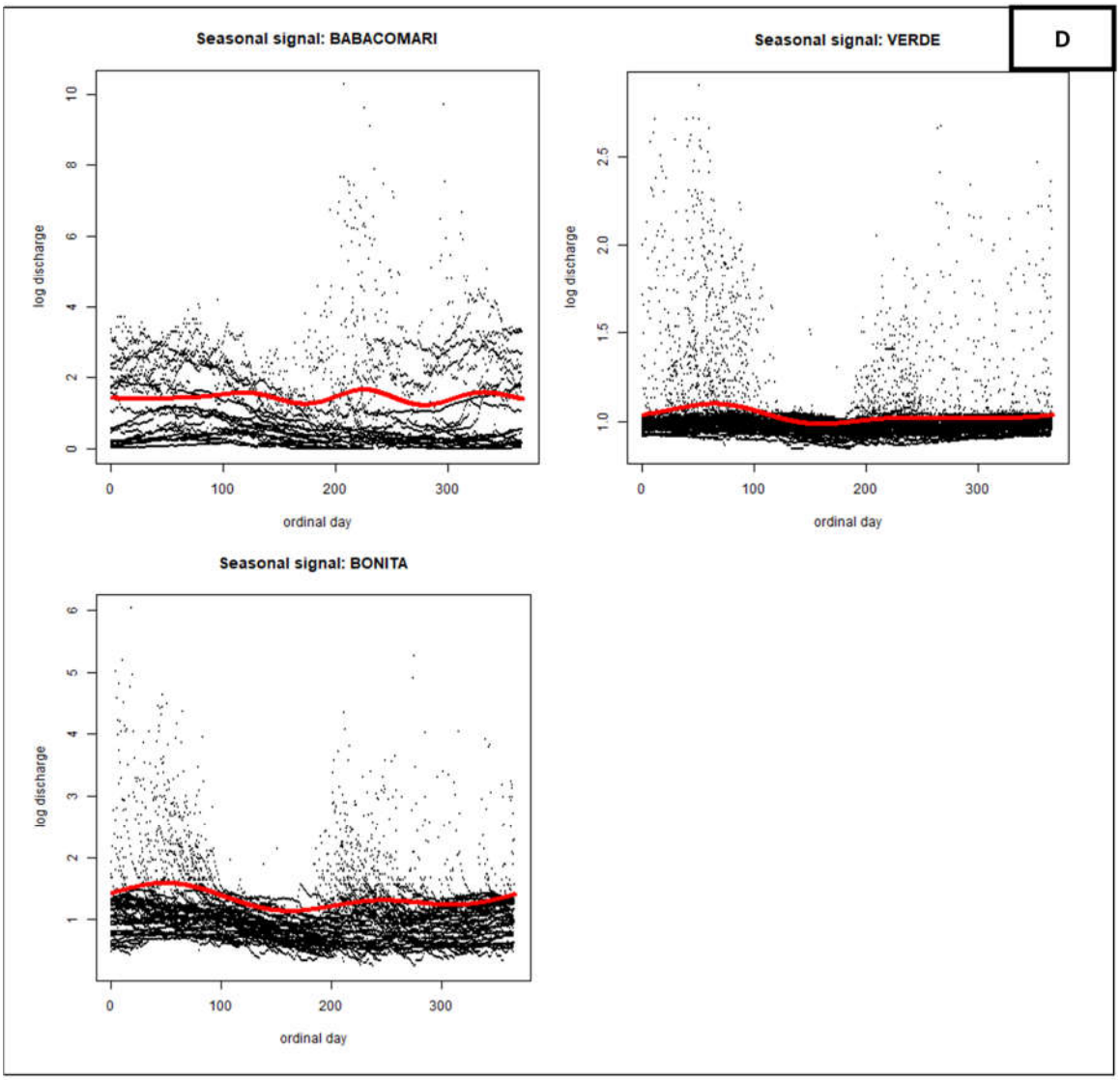

Hydrologic regimes and regime shifts

Discrete Fast Fourier Transform (DFFT) was applied to describe both intra-annual and inter-annual difference in streamflow for the past 20 years - the former is illustrated by the timing and magnitude of the annual extreme residuals (Figure 4 a, b, c, and d), whereas the later represents departures from the long-term hydrologic trend- anomalies (Figure 4 A, B, C, and D). The exact timing the annual extreme residuals in each year (Figure 4 a, b, c, and d) corresponds but does not

necessarily match seasonal discharge signal of each hydrological categories (Figure 3). For example, for a stream in the “winter” group, only some of the annual extreme residuals appeared in winter but most happened in March and April (Table S1 and Figure S1 in the Appendix). For the year-to-year variations, the 20-year period encompassed both wet and dry periods in all sites (Figure 4 A, B, C, and D). Some sites, like Wet Beaver Creek, San Pedro River, and San Francisco River, experienced more frequent transitions between negative flow anomalies (dry regime) and positive flow anomalies (wet regime), with relatively short intervals between each hydrologic regime shift.

Wavelet analysis showed that there were numerous hydrologic regime shifts in most of the time series (Figure S2 in the Appendix). The annual power maxima of Wet Beaver Creek and San Pedro River provide a comparison between systems with varied frequency of hydrologic regime shifts and different consistency of return intervals (Figure 5). Additionally, antecedent hydro-climatic conditions have a strong lagged autocorrelation (memory), that significantly impacted the peaks of flood waves. The memory effect also differed in these streams.

Figure 4: DFFT result. a, b, c, and d: Annual extreme residuals of discharge along time (X axis: year; Y axis: Residual event magnitude; dash line: low-flow event magnitude equal to 2 sigma; dotted line: high-flow event magnitude equal to 2 sigma; empty square: annual extreme high-flow residuals; empty dot: annual extreme low-flow residuals. A, B, C and D: Net annual anomalies (red: dry regime with negative NAA; blue: wet regime with positive NAA) and delta net annual anomalies of each year (red: dry regime without regime shift; green: regime shift from dry to wet; blue: regime shift from wet to dry; purple: wet regime without regime shift). One stream was chosen as an example for each subset. A and a: Winter; B and b: Summer; C and c: Bimodal; D and d: Flashy. See Figure S1 in the Appendix for the full result.

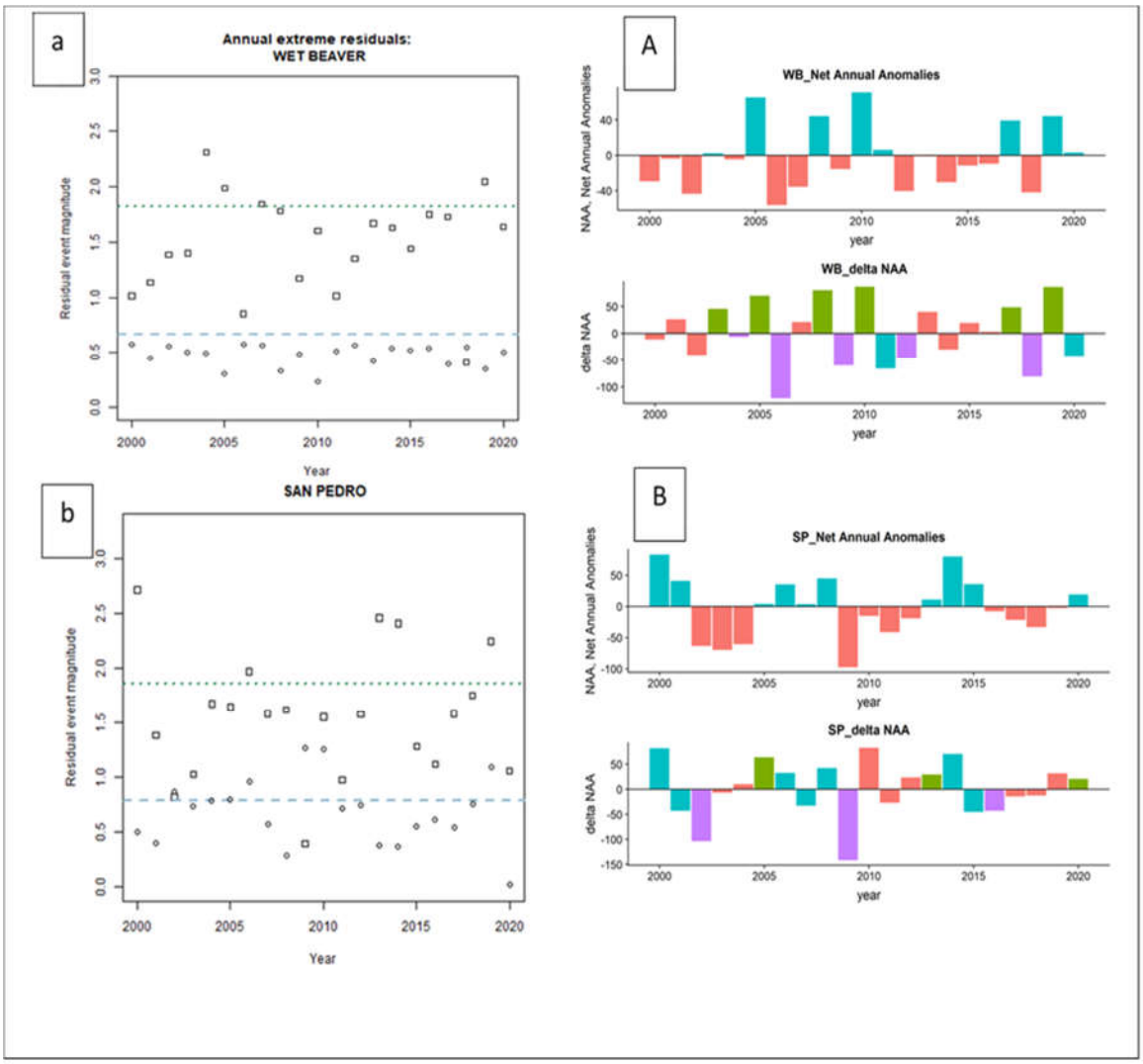

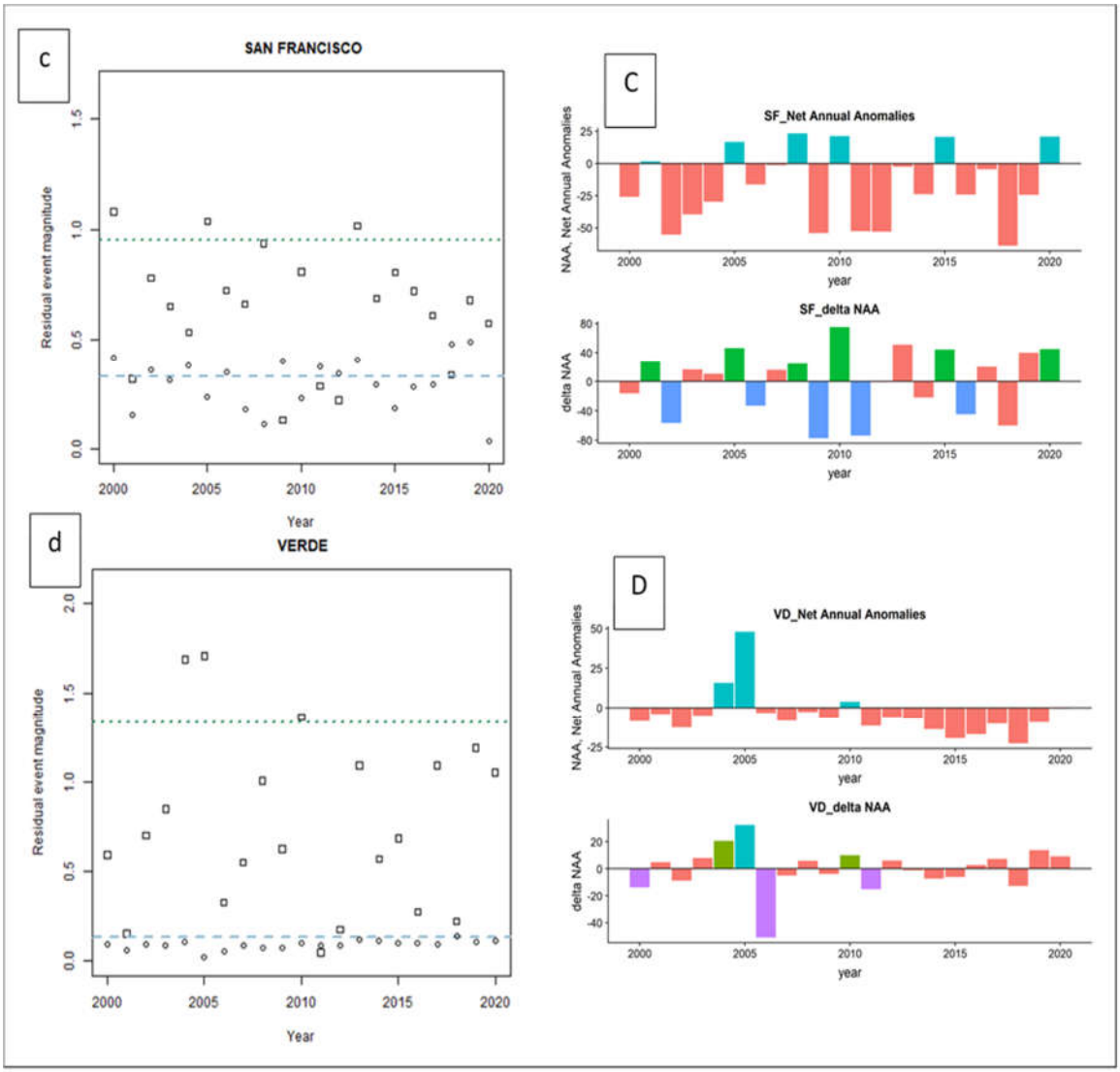

Figure 5: Scale-average time series of max annual aggregate blue noise power along time, using Wet Beaver and San Pedro rivers as two examples. X axis: year, Y: aggregate blue noise power. See Appendix Figure S2 for full result.

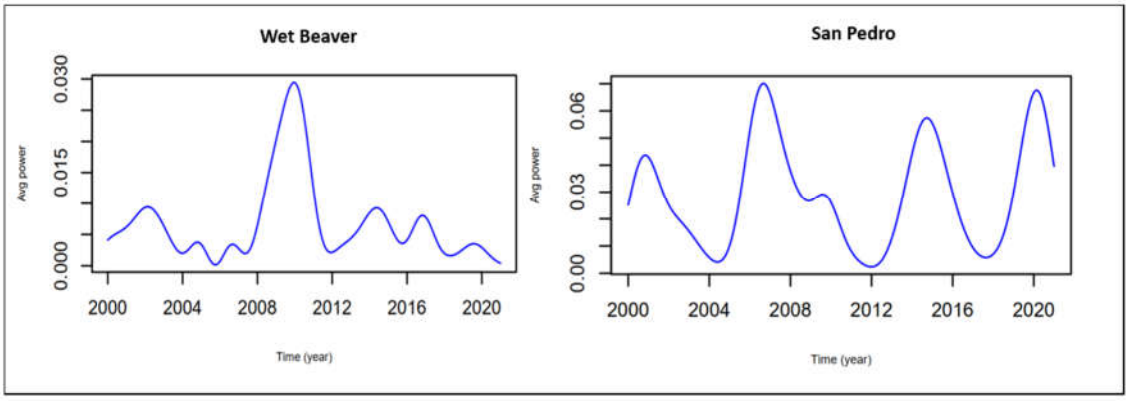

Drivers of spatiotemporal variation in stream metabolism

Controls on the seasonal mean GPP and ER

PCA on the seasonal mean of water chemistry parameters showed that the first two principal components combined (PC1 and PC2) explained around 43% of the variance in the water chemistry dataset and were used for next step multiple linear regression analysis (Table 4 A and B). PC1 was negatively correlated with all the seasonal mean of concentration (sodium -0.455, potassium -0.438, chloride -0.397, etc). PC2 was positively correlated with some variables like chloride (0.374) and DOC (0.362), and negatively correlated with some others like Ammonium (-0.448). No strong correlation was found between net seasonal anomaly and seasonal sum of aggregate blue noise power (p=0.594), and they were both included in the MLR model. The result indicated that the second principal component (PC2) of water chemistry parameters and water depth were strong predictors of GPP (adjusted R^2=0.3512), while water depth was one of the most significant predictors of ER (adjusted R^2=0.555, Table 5). Furthermore, individual nutrient concentration variables were explored, and I found that GPP was significantly correlated with nitrate concentration, SRP concentration, water depth, temperature, and PAR (adjusted R^2=0.626, Table 7). For ER, nitrate concentration, temperature, and depth were significant predictors of ER (adjusted R-squared=0.652). Neither the aggregate blue noise power nor the net seasonal anomaly was found to correlated with GPP. Only seasonal mean of ER responded to blue noise power.

Table 4 A: PCA result: the first 3 principal components of seasonal mean of water chemistry variables.

Importance of components	PC1	PC2	PC3
Standard deviation	1.779	1.249	1.203
Proportion of Variance	0.288	0.142	0.132
Cumulative Proportion	0.288	0.430	0.561

Table 4 B: The matrix of seasonal mean of water chemistry variable loadings

	PC1	PC2	PC3
SRP_mean	-0.330	0.483	-0.116
DOC	-0.288	0.532	0.060
Fluoride	-0.124	0.084	0.148
Chloride	-0.440	0.012	0.316
Sulfate	-0.303	0.059	-0.414
Nitrate	-0.124	-0.374	-0.120
Sodium	-0.476	-0.316	0.148
Ammonium	-0.077	-0.007	-0.650
Potassium	-0.445	-0.105	0.135
Magnesium	-0.186	-0.462	-0.001
Calcium	-0.165	-0.095	-0.462

*Table 5: MLR result using mean GPP and ER as response variables. Hypothesized predictor variables with * have statistically significant association with the response variable, with p <0.05.*

response variable	Predicted variables	Coefficients Estimate	Std. Error	t value	Pr(>|t|)	Adjusted R-squared	F-statistic p-value
Mean GPP	(Intercept)	-1.48E+00	1.36E+00	-1.091	0.279822	0.3512	1.83E-05
	PC1_waterchem	-5.14E-03	1.64E-01	-0.031	0.975111		
	PC2_waterchem***	-7.01E-01	1.96E-01	-3.567	0.000717		
	temp.water_mean	1.26E-01	7.39E-02	1.71	0.092483		
	light_median	1.63E-03	1.28E-03	1.268	0.209654		
	depth_mean**	4.74E+00	1.72E+00	2.752	0.007827		
	NSA	1.17E-03	8.98E-03	0.13	0.897241		
	sumpower.seasonal	-4.45E-07	3.29E-05	-0.014	0.989257		
Mean GPP	(Intercept).	-1.68E+00	9.10E-01	-1.841	0.070602	0.6261	3.56E-12
	DOC.	5.26E-03	2.91E-03	1.805	0.076026		
	Nitrate***	5.28E-02	7.18E-03	7.347	6.38E-10		
	SRP_mean***	-1.63E+00	3.99E-01	-4.095	0.000128		
	temp.water_mean*	1.29E-01	5.00E-02	2.578	0.012404		
	light_median*	2.41E-03	9.62E-04	2.506	0.014952		
	sumpower.seasonal	-2.13E-05	2.59E-05	-0.824	0.413387		
	depth_mean**	4.14E+00	1.30E+00	3.19	0.002265		
Mean ER	(Intercept)	1.24E+00	1.39E+00	0.894	0.3748	0.555	5.22E-10
	PC1_waterchem	1.15E-01	1.68E-01	0.686	0.4952		
	PC2_waterchem*	4.51E-01	2.01E-01	2.247	0.0284		
	temp.water_mean*	-1.67E-01	7.54E-02	-2.213	0.0307		
	light_median	-5.76E-04	1.31E-03	-0.44	0.6616		
	depth_mean***	-1.14E+01	1.76E+00	-6.485	1.88E-08		
	sumpower.seasonal.	6.50E-05	3.36E-05	1.935	0.0577		
	NSA	1.16E-02	9.17E-03	1.267	0.21		
Mean ER	(Intercept)	1.66E+00	1.08E+00	1.535	0.12996	0.652	4.49E-13
	DOC	-4.66E-03	3.47E-03	-1.345	0.18376		
	Nitrate***	-4.38E-02	8.55E-03	-5.125	3.34E-06		
	SRP_mean	7.60E-01	4.74E-01	1.603	0.11427		
	temp.water_mean**	-1.60E-01	5.94E-02	-2.684	0.00939		
	light_median	-1.54E-03	1.15E-03	-1.343	0.18419		
	sumpower.seasonal*	7.65E-05	3.08E-05	2.487	0.01566		
	depth_mean***	-1.08E+01	1.54E+00	-7.004	2.46E-09		

Controls on the variance of stream metabolism

PCA on the CV of water chemistry parameters showed that PC1 was positively correlated with the CV of calcium (0.312), potassium (0.136) and sulfate (0.051), and negatively correlated with the CV of all other parameters (SRP, DOC, fluoride, chloride, nitrate, sodium, ammonium, and magnesium). The first principal component combined explained almost 30% of the variance in the water chemistry dataset and was selected for next step analysis (Table 6A and 6B). Another PCA was run on the hydrologic variables and the first principal component combined explained over 60% of the variance in the hydrological dataset and was selected for next step analysis (Table 6C and 6D). PC1 was negatively correlated with LSAM (-0.323), HSAF (-0.283), LSAF (-0.284) and snr (-0.108), and positively correlated with all other parameters, like HFsigma (0.383), LFsigma (0.379), FPExt (0.363) etc.

Furthermore, linear regression model specifically demonstrated that size had no control over CV of concentrations of them (p=0.992), nor was it associated with CV of local environmental factors like water temperature (p=0.680) and PAR (p=0.909), but size, represented by the watershed area was significantly corelated with hydrological variability (p=0.047) (Table 7).

Lastly, the multiple linear regression models revealed that CV of GPP was driven by the first principal component of water chemistry parameters, size (watershed area) and CV of PAR (Table 8). More specifically, CV of SRP and CV of nitrate concentration and CV of PAR were significantly corelated with CV of GPP. PC1 of hydrology is the only factor found to be associated with the CV of ER.

Table 6 A: PCA results: the first 3 principal components of coefficient of variation of water chemistry parameters

Importance of components	PC1	PC2	PC3
Standard deviation	1.796	1.598	1.299
Proportion of Variance	0.293	0.232	0.153
Cumulative Proportion	0.293	0.525	0.679

Table 6 B: The matrix of chemistry variable loadings

	PC1	PC2	PC3
SRP	-0.412	-0.348	0.027
DOC	-0.084	-0.519	0.009
Fluoride	-0.307	0.386	-0.329
Chloride	-0.285	0.286	0.343
Sulfate	0.051	0.219	0.468
Nitrate	-0.265	0.484	-0.022
Sodium	-0.479	-0.080	0.076
Ammonium	-0.042	0.045	0.478
Potassium	0.136	-0.121	0.555
Magnesium	-0.477	-0.265	0.013
Calcium	0.312	-0.053	-0.107

Table 6 C: PCA result: the first 3 principal components of hydrological variables

Importance of components	PC1	PC2	PC3
Standard deviation	2.499	1.426	0.994
Proportion of Variance	0.624	0.203	0.099
Cumulative Proportion	0.624	0.828	0.927

Table 6 D: The matrix of chemistry variable loadings

	PC1	PC2	PC3
aggregate.power	0.269	0.376	-0.152
HSAM	0.373	0.113	-0.218
LSAM	-0.323	-0.373	-0.123
HSAF	-0.283	0.434	-0.301
LSAF	-0.284	0.399	-0.288
FPExt	0.363	0.285	0.083
NAAmean	0.300	-0.170	0.435
HFsigma	0.383	-0.087	-0.167
LFsigma	0.379	0.018	-0.293
snr	-0.108	0.491	0.657

*Table 7: LR result exploring the correlation between size (watershed area) and other predicted variables. Predicted predictor variables with * have statistically significant association with size, with p <0.05*

Independent variable	Dependent variable	adj.r.squared	Intercept	Slope	P-value
area	PC1_waterchem	-0.111	-0.005	0	0.993
	PC1_hydro*	0.301	1.304	-0.001	0.047
	temp.water_cv	-0.089	19	0	0.68
	light_cv	-0.109	182.8	0	0.909

*Table 8: MLR result using CV of GPP and ER as response variables. Predicted predictor variables with * have statistically significant association with the response variable, with p <0.05.*

Response variable	Predicted variables	Coefficients Estimate	Std. Error	t value	Pr(>|t|)	Adjusted R-squared	F-statistic p-value
CV of GPP	(Intercept)	-65.395	45.837	-1.427	0.213	0.781	0.0192
	PC1_waterchem *	-11.235	4.017	-2.797	0.038		
	PC1_hydro	-0.984	3.195	-0.308	0.771		
	area*	-0.008	0.003	-2.814	0.037		
	temp.water_cv	-1.715	1.44	-1.191	0.287		
	light_cv*	1.127	0.366	3.084	0.027		
CV of GPP	(Intercept)*	-285.5	88.1	-3.24	0.0317	0.825	0.02674
	Nitrate_cv*	0.8628	0.3084	2.798	0.0489		
	SRP_mean_cv*	1.087	0.3149	3.453	0.026		
	PC1_hydro	-5.016	2.968	-1.69	0.1663		
	area	-0.004967	0.002804	-1.771	0.1512		
	temp.water_cv	-7.062	2.63	-2.685	0.0549		
	light_cv*	1.977	0.4962	3.985	0.0163		
CV of ER	(Intercept)	146.586	119.439	1.227	0.266	0.527	0.072
	PC1_waterchem	6.107	10.118	0.604	0.568		
	PC1_hydro*	-16.635	6.342	-2.623	0.039		
	temp.water_cv	-0.404	3.745	-0.108	0.918		
	light_cv	-1.215	0.947	-1.283	0.247		
CV of ER	(Intercept)	93.8029	223.5017	0.42	0.6921	0.5743	0.08878
	Nitrate_cv	0.4489	0.7769	0.578	0.5885		
	SRP_mean_cv	-0.4518	0.7547	-0.599	0.5755		
	PC1_hydro	-17.8544	7.5318	-2.371	0.0639		
	temp.water_cv	-3.2109	6.8547	-0.468	0.6592		
	light_cv	-0.7652	1.3297	-0.575	0.5899		

DISCUSSION

Streams and rivers are active processors of and/or substantial sinks for carbon, and the global carbon budget needs to consider including these fluxes (Cole et al. 2007; Battin et al. 2008, 2009). According to Griffiths et al. (Griffiths et al 2013) and Battin et al. (2009), terrestrial carbon flux to inland waters is either respired and released as atmospheric CO_2 (50%) or stored in sediments (33%). Further, 25% of the total flux was estimated to be the CO_2 evasion from streams and rivers (Battin et al. 2008). Hence, understanding the variance on gross primary production (GPP), ecosystem respiration (ER), and net ecosystem production (NEP) of the fluvial ecosystems is of great importance. In addition to connecting stream ecology to global carbon fluxes, stream metabolism is a critical indicator of ecosystem health with significant influences on ecosystem functioning (Fellows et al., 2006; Correa-González et al., 2014). Stream metabolism also has multiple implications for ecological processes. For instance, stream metabolism affects secondary productivity by affecting the nutritional resource quality for consumers in the food chains (Boëchat et al., 2011). Anthropogenic influences on metabolism may change nitrogen and phosphorus retention (Gücker and Pusch, 2006; Merseburger et al., 2011) as well as organic matter processing (Tank et al., 2010). These biogeochemical changes are important to drinking-water quality and pollution abatement, which are important ecosystem services that rivers and streams provide (Hall and Tank, 2003; Sobota et al., 2012). There has been a long and rich history of studies on the rates and controls on stream metabolism owing to its ecological importance. As a result, ecologists have

gained some insight by comparing metabolic rates and some hypothetical factors among streams and rivers (e.g., Mulholland et al., 2001; Bernot et al., 2010; Hoellein et al., 2013). However, due to the diverse and dynamic nature of rivers and streams and their complex linkages with the surrounding terrestrial ecosystems, no universal or regional controlling factors on stream metabolism have yet been concluded (Bernhardt et al. 2018).

This study provided one of the most comprehensive analyses of stream metabolism currently available in the southwestern US desert and mountainous area, as these sites span diverse regions and share similarities and dissimilarities in hydroclimatic conditions that potentially influence GPP and ER. Using a significant spatial gradient in stream order (size) and hydrologic variability, I focused on the variation (CV) of both explanatory and response variables and how variation in drivers (hydrology, nutrient concentrations, local environment and size) may affect variation in response (photosynthesis and respiration). These predicted variables represent the difference of disturbance regime in magnitude, timing and frequency within the catchment and the stability of local environment in terms of the temperature and PAR, while the variations of GPP and ER are important indicators for evaluation of stability at the ecosystem level.

As a result, I found that: 1) although vast variation in hydrologic variability was observed across 11 streams (Figure 3, 4, 5 and Appendix Figure S1, Figure S2 and Table S1) both interannually and intra-annually (seasonally), hydrologic variation only predicted the CV of ER but not the CV of GPP. The CV of photosynthesis and respiration responded differently to discharge anomalies representing hydrologic variability. 2) The variability in nutrient supply and PAR were the dominant

controls on the CV of GPP but not ER, while the CV of water temperature was not associated with CV of GPP or ER at all. 3) Watershed area, representing the size of study rivers and streams, was correlated with the hydrologic variability but not with the CV of local environment (water temperature and PAR) or CV of nutrient loadings. Size only predicted the CV of GPP but not CV of ER. Additionally, the seasonal dynamic of stream metabolism was also illustrated by repeated short-term (mostly <7 days) measurement of GPP and ER. The analysis of the effects of nutrient concentration, PAR, water temperature, hydrology and water depth on seasonal averaged estimates of GPP and ER revealed the following findings: 1) hydrologic condition was not correlated with GPP but with ER. 2) Nitrate concentration and water depth were both strong predictors on GPP and ER. 3) PAR predicted GPP whereas water temperature predicted GPP and ER. 4) Water depth was a strong determinant of both GPP and ER. Generally, the findings revealed in my research are consistent with previous studies, but I also noted several major differences between my study and others already published which will be discussed as following.

Seasonal stream metabolism in aridland and the CV of stream metabolism

The range of daily GPP and ER rates presented in my study are similar to those of previous research. Mulholland et al. (2001) reported GPP ranging from <0.1- 15 g $O_2m^{-2}d^{-1}$ and ER ranging from 2.4-11 g $O_2m^{-2}d^{-1}$ for 11 streams across the continental US. The NEP was reported negative for all streams except Sycamore Creek. Six of the eight streams were strongly heterotrophic, with P to R ratios below 0.25 (Mulholland et al. 2001). Noted by Marzolf and Ardón (2021), across all 202 GPP and ER measurements from 83 streams and rivers across the global tropics, median GPP

was 0.4 g $O_2m^{-2}d^{-1}$ (ranging from 0.01 to 11.7 g $O_2m^{-2}d^{-1}$) and median ER was 4.30 g $O_2m^{-2}d^{-1}$ (range from 0.1 to 42.1 g $O_2m^{-2}d^{-1}$). Similarly, these streams were predominately heterotrophic with NEP being negative; in other words, GPP being lower than ER. In my study of 11 aridland streams and rivers located in the southwestern US, seasonal GPP and ER and their CV were all in the range mentioned in the existing literature. In only 14 of 95 measurements (14.74%) was GPP higher than ER, including seven in the cool winter rainy season (1st quarter), three in the pre-monsoon season (2nd quarter), three in the late fall-winter (4th quarter), and only one in the monsoon season (3rd quarter). Sycamore Creek was reported to be autotrophic during summer (Grimm and Fisher, 1984) and I found this stream was autotrophic in 1st quarter 2017, but heterotrophic the rest of the time. Only 29 of 81 (36%) of measurements were strongly heterotrophic with P to R ratios lower than 0.25. This percentage is slightly lower than that found in previous studies (Bernot et al. 2010). In other word, the selected streams and rivers have notably higher P to R ration in general and hence may differ from closed canopy and less flashy river systems already studied.

Features of hydrologic variation of aridland streams

Aridland streams and rivers are hydrologically diverse and dynamic (Sabo and Post, 2007; Cooper et al. 2013). Although all located in the desert Southwest in Arizona, these streams demonstrate similarities and dissimilarities from site to site and from time to time in terms of the seasonality and anomalies of streamflow. The hydrological category is a novel concept proposed in my study, with the purpose of showing variation with respect to the form of the seasonal signal of rainfall and hence discharge. This will also help to distinguish the efficiency of summer monsoon and winter

frontal storms in generating streamflow in aridland streams. The hydrological features of these streams were interpreted using the seasonal signal of flow from a different angle of some existing studies. For instance, Blasch et al. reported clear winter peaks in Upper Verde River in 2006 (Blasch et al. 2006) though I did not detect strong seasonal signal. Furthermore, the timing of the hydrologic variability was represented by filtering out the annual extreme residuals in each calendar year. The annual extreme residuals did not necessarily occur in the season(s) anticipated to have floods. For instance, as a winter-frontal dominated stream, Sycamore Creek often had its annual extreme residuals in the winter rain season from January to March (52%) and sometimes from July to September (i.e., monsoon, 29%) or from October to December (19%). Santa Cruz River was dominated by summer monsoon, and 76% of the peak events happened from July to September. These streams and rivers also show evident difference in terms of the net annual anomalies. Some streams experienced frequent hydrological regime shifts in the recent 2 decades record, like Wet Beaver Creek and San Francisco River, which both had six shifts from dry regime to wet regime and five from wet regime to dry regime. Some others like Verde River only saw two shifts from dry regime to wet regime and two from wet regime to dry regime. In addition to regime-shift frequency, wavelet analysis also provides insight into hydrological regime shifts. Significant blue noise signals showed the transitions between different regimes. The time series of maximum annual blue noise power at scales of 1-2 years was plotted to demonstrate the clear qualitative differences in the wavelet spectra of flow from different streams and rivers. This, along with DFFT, is an important and initial step to identify, characterize and classify the hydroclimatic regimes of stream flow.

Hydrology predicting ER but not GPP

GPP and ER and their CVs responded differently to hydrological variability. Neither GPP nor the CV of GPP was correlated with the hydrologic regime or high-flow parameters, but ER and the CV of ER did respond to hydrological variation. This research is novel as we focused on the impact of varied hydrologic regime, frequency, timing, and magnitude of regime shifts instead of discharge itself. Some studies within individual streams (e.g., Mulholland et al., 2001; Bernot et al., 2010) and syntheses across sites (Hoellein et al., 2013) concluded that hydrologic disturbance impacts organic matter transport and hence the accumulation and temporal attributes of hydrologic variation describing the magnitude, duration, timing, and frequency of extreme events are predicted to associate with metabolism in streams. Floods and droughts have been considered as the main formats that hydrologic variations contribute to the temporal variation in stream metabolism. Floods may scour biofilms and streambed, reduce light availability to algae, and change the abundance of biota including benthic algae (Fisher et al. 1982; Power and Stewart, 1987; Grimm and Fisher 1989). Also, increased streamflow can elevate DOC concentrations, which may lead to reduced GPP due to light attenuation (Leggieri et al., 2013). Droughts and river drying, though receiving far less attention, cause mortality of primary producers. Additionally, streams with unstable sediments such as sand are especially sensitive to increased discharge and they usually have low production rates according to a study by Hondzo et al (2013). As a result, aridland streams experiencing frequent hydrologic disturbances can have a relatively low GPP and high ER. In my study, stream ER was stimulated by hydrological events, and the CV of ER was negatively correlated with discharge

anomalies. Although the decrease in biomass and metabolism after floods events in aridland streams has been previously reported (Fisher et al. 1982, Vilches and Giorgi, 2010; Acuña et al., 2011), I did not find evidence that the rate and variability of seasonal GPP responded to the stability of hydrological condition over long term (annual or longer scale). It is likely because, on the one hand, the memory effect of extreme hydrological events on primary production is muted as the impact does not last long in aridland streams due to the extremely dynamic nature. On the other hand, DFFT and wavelet methods—which quantify the features of hydrologic regimes at annual and decadal scales—do not consider shorter-term hydrologic variation, which does not match the scale of stream metabolism and the variation of GPP and ER. In other words, change of GPP and ER in response to hydrologic events occurred in days (O'Connor et al., 2012) and hence, the daily variation of metabolism would be necessary to detect the association with short-term hydrologic characteristics. This study lacks high-resolution temporal metabolism data that would be required and therefore cannot fully test the role of hydrologic variation in controlling daily metabolism.

PAR correlated with GPP and temperature correlated with ER

The local environmental variables water temperature and PAR appear to be be strong determinants of mean and CV of stream metabolism across 11 aridland streams. Significant association was detected between PAR and GPP, and between CV of PAR and CV of GPP as well. This finding agrees with other studies of stream metabolism (Naiman, 1983; Bott et al., 1985; Young & Huryn, 1999, Mulholland et al., 2001). Small headwater streams with a high proportion of canopy cover often have high light intensity and duration of daylight, primarily as a result of the lower density of

riparian vegetation found in arid and semi-arid regions. Streams with high percentage of canopy cover usually receive seasonally different amount of light as the leaves emerge and shade the stream in summer and autumn, leading to seasonality of GPP in the streams covered by canopy (Mulholland et al. 2000). Temperature was confirmed to have a modest effect on ER in my study. But the CV of ecosystem respiration wasn't significantly associated with the CV of temperature. The study by Bott et al. (1985) found temperature being "the best single predictor of R", which explained 33% of the variation in respiration of streams across four different biomes in US. At an annual scale, mean temperature was found to explain 38% of the variation in mean ER in a comparative study of 22 streams (Sinsabaugh 1997). Streams with high variance of water temperature should have increased likelihood to observe an effect on ER (Mulholland et al. 2001, Perkins et al. 2012). Although hard to be detected as in Arizona, as the temperature range from site to site is relatively narrow, this finding supported water temperature as a predictor of ER.

Nutrient concentrations determining GPP and ER

In my project, nitrate concentration was found to be strongly associated with ER while concentrations of nitrate and SRP both were strong predictors of GPP. The CV of GPP was also attributed to the CV of the PC1 of all water chemistry parameters. In literature, nutrient concentration and availability (e.g., Grimm and Fisher, 1984; Gausch et al., 1995) together with the quantity and quality of organic matter (e.g., Webster et al., 1997) are important predictors of ER. Few studies found out that the increasing nitrate concentrations affects the efficiency of biotic uptake and nitrate denitrification, as related to photosynthetic production and respiration (Peterson

et al. 2001; Duff et al. 2008; Mulholland et al. 2008). The detailed explanation is, the increased availability of carbon favors the immobilization- nutrient uptake by heterotrophic microbes, and the increase in the carbon and nutrient usually leads to an increase in heterotrophic activity and a decrease in oxygen concentration due to respiration. As a result, the anaerobic environment can foster denitrification (Grimm 2005). In aridland streams, sometimes the benthic production could fuel over 80% of the hyporheic respiration through dissolved material leaching (Jones et al. 1995). Highly varied precipitation dictates nutrient status of stream ecosystems and nutrient received by streams from the surrounding catchment. In this case, concentration of nutrient and organic matter should be one of the determinants of the metabolic rate of streams.

Water depth driving stream metabolism and watershed area driving CV of GPP

Lastly, watershed area (size) was driving the hydrologic regime and CV of GPP, as expected. But it was not a significant driver of CV of ER, CV of nutrient concentrations, or CV of local environmental factors including PAR and temperature. Although not supported by this data, some existing literature indicated that large catchments are usually associated with high ER due to a higher drainage of nutrients and carbon, while canopy shading and hydrologic disturbance are believed to decline between small streams and large rivers (e.g., Marzolf and Ardón, 2021; Finlay, 2011; Hoellein et al., 2013; Howarth & Sherman, 1991). Water depth, although not correlated with temperature or light, was a strong predictor on point measurement of GPP and ER.

CONCLUSION

To conclude, 11 aridland streams in Southwest US- Arizona across a hydroclimatic and size (watershed area) gradient were surveyed. The seasonal averaged GPP ranged from 0.001 g $O_2m^{-2}d^{-1}$ to 4.6 g $O_2m^{-2}d^{-1}$ and ER from 0.0026 g $O_2m^{-2}d^{-1}$ to 20 g $O_2m^{-2}d^{-1}$. It was concluded that hydrologic variation only predicted the ER and CV of ER but not the GPP or CV of GPP; PAR and its CV controlled GPP and its CV respectively whereas temperature was one of the controller on ER; CV of nutrient concentration was one of the drivers of CV of GPP, nitrate concentration was correlated with point measurement of GPP and ER while SRP concentration was only relevant to GPP; watershed area was correlated with CV of GPP, while depth mattered to both GPP and ER. Generally, most of these findings concerning the predictors on GPP and ER were consistent with previous studies, but it is also noted that several differences existed between my study and others already published conclusions and some guesses were made to explain such inconsistency. The study system- 11 streams and rivers in arid and semi-arid region in Southwest US are highly dynamic and share lots of similarities and dissimilarities, with notably higher P:R in general. Additionally, the focused of this work was the variation of variables, and how variation in response variables (the rate of photosynthesis and respiration) responded to the variation in explanatory variables, which hasn't been thoroughly explored in existing literature. Admittedly, there are some limitations in this study. For example, short-term features of the discharge variations need to be further explored and linked to the variation of stream metabolism. The metabolism model has

limited capacity and accuracy in predicting the GPP and ER when the diurnal GPP-driven O_2 signal was weak. Short-term (mostly <7 days) repeated measurements of metabolism were used to capture seasonal dynamics and that provided limited information on the spatiotemporal variation in photosynthetic productivity and ecosystem respiration in aridland streams (Ulseth et al., 2019; Savoy et al., 2019; Bernhardt et al., 2018). The next step movement would be to utilize the continuous monitoring data from StreamPULSE project to model daily GPP and ER, analyze the temporal and spatial features with time series methods that are time-scale appropriate and further address the linkages between the changing controls and changing stream metabolism.

The visualization of hydrologic features and stream metabolism can better inform our understanding of streams at the multiple temporal and spatial scale and ultimately river management practice (Fausch et al. 2002, Naiman et al. 2012, Saunders et al. 2018). Resolving how changes and variations in the abiotic conditions like hydrology, temperature, PAR, nutrient loadings may drive changes and variations in biotic responses of GPP and ER is one essential step in the understanding the complex patterns of metabolic regimes (Bernhardt et al., 2017). This work reveals that aridland streams could be vulnerable to discharge alteration related to flow regime shifts under global climate change and anthropogenic activities, and alteration of nutrient loading leading to further dissolved oxygen consumption. Such impact at the base of the food web has great implications for ecosystem functioning and upper level of food webs in streams.

REFERENCES

Acuña, V. (2004). Riparian forest and hydrology influences on the ecosystem structure and function of a Mediterranean stream.

Acuña, V., Giorgi, A., Muñoz, I., Uehlinger, U., & Sabater, S. (2004). Flow extremes and benthic organic matter shape the metabolism of a headwater Mediterranean stream. Freshwater biology, 49(7), 960-971.

Acuña, V., Giorgi, A., Muñoz, I., Uehlinger, U. R. S., & Sabater, S. (2004). Flow extremes and benthic organic matter shape the metabolism of a headwater Mediterranean stream. Freshwater biology, 49(7), 960-971.

Acuña, V., Vilches, C., & Giorgi, A. (2011). As productive and slow as a stream can be—the metabolism of a Pampean stream. Journal of the North American Benthological Society, 30(1), 71-83.

American Public Health Association, & American Water Works Association. (1995). Standard methods for the examination of water and wastewater. In Standard methods for the examination of water and wastewater (pp. 1000-1000).

Appling, A. P., Hall Jr, R. O., Yackulic, C. B., & Arroita, M. (2018). Overcoming equifinality: Leveraging long time series for stream metabolism estimation. Journal of Geophysical Research: Biogeosciences, 123(2), 624-645.

Appling, A. P., Hall, R. O., Yackulic, C. B., & Arroita, M. (2018). Overcoming Equifinality: Leveraging Long Time Series for Stream Metabolism Estimation. Journal of Geophysical Research: Biogeosciences, 123(2), 624-645. doi:10.1002/2017jg004140

Battin, T. J., Kaplan, L. A., Findlay, S., Hopkinson, C. S., Marti, E., Packman, A. I., . . . Sabater, F. (2008). Biophysical controls on organic carbon fluxes in fluvial networks. Nature Geoscience, 1(2), 95-100.

Battin, T. J., Luyssaert, S., Kaplan, L. A., Aufdenkampe, A. K., Richter, A., & Tranvik, L. J. (2009). The boundless carbon cycle. Nature Geoscience, 2(9), 598-600.

Beaulieu, J. J., Arango, C. P., Balz, D. A., & Shuster, W. D. (2013). Continuous monitoring reveals multiple controls on ecosystem metabolism in a suburban stream. Freshwater biology, 58(5), 918-937.

Bernhardt, E. S., Blaszczak, J. R., Ficken, C. D., Fork, M. L., Kaiser, K. E., & Seybold, E. C. (2017). Control points in ecosystems: moving beyond the hot spot hot moment concept. Ecosystems, 20(4), 665-682.

Bernhardt, E. S., Heffernan, J. B., Grimm, N. B., Stanley, E. H., Harvey, J. W., Arroita, M., . . . Hall Jr, R. O. (2018). The metabolic regimes of flowing waters. Limnology and Oceanography, 63(S1), S99-S118.

Bernot, M. J., Sobota, D. J., Hall Jr, R. O., Mulholland, P. J., Dodds, W. K., Webster, J. R., . . . Dahm, C. N. (2010). Inter ‐ regional comparison of land ‐ use effects on stream metabolism. Freshwater biology, 55(9), 1874-1890.

Bernot, M. J., Sobota, D. J., Hall, R. O., Mulholland, P. J., Dodds, W. K., Webster, J. R., . . . Wilson, K. Y. M. (2010). Inter-regional comparison of land-use effects on stream metabolism. Freshwater biology, 55(9), 1874-1890. doi:10.1111/j.1365-2427.2010.02422.x

Blasch, K. W., Hoffmann, J. P., Graser, L. F., Bryson, J. R., & Flint, A. L. (2006). Hydrogeology of the upper and middle Verde River watersheds, central Arizona. Retrieved from

Boëchat, I. G., Krüger, A., Giani, A., Figueredo, C. C., & Gücker, B. (2011). Agricultural land-use affects the nutritional quality of stream microbial communities. FEMS Microbiology Ecology, 77(3), 568-576.

Bott, T. L., Brock, J. T., Dunn, C. S., Naiman, R. J., Ovink, R. W., & Petersen, R. C. (1985). Benthic community metabolism in four temperate stream systems: an inter-biome comparison and evaluation of the river continuum concept. Hydrobiologia, 123(1), 3-45.

Carpenter, B., Gelman, A., Hoffman, M. D., Lee, D., Goodrich, B., Betancourt, M., . . . Riddell, A. (2017). Stan: A probabilistic programming language. Journal of statistical software, 76(1), 1-32.

Cazelles, B., Chavez, M., Berteaux, D., Ménard, F., Vik, J. O., Jenouvrier, S., & Stenseth, N. C. (2008). Wavelet analysis of ecological time series. Oecologia, 156(2), 287-304.

Cole, J. J., Caraco, N. F., & Peierls, B. (1991). Phytoplankton primary production in the tidal, freshwater Hudson River, New York (USA). Internationale Vereinigung für theoretische und angewandte Limnologie: Verhandlungen, 24(3), 1715-1719.

Cole, J. J., Carpenter, S. R., Kitchell, J., Pace, M. L., Solomon, C. T., & Weidel, B. (2011). Strong evidence for terrestrial support of zooplankton in small lakes based on stable isotopes of carbon, nitrogen, and hydrogen. Proceedings of the National Academy of Sciences, 108(5), 1975-1980.

Cole, J. J., Prairie, Y. T., Caraco, N. F., McDowell, W. H., Tranvik, L. J., Striegl, R. G., . . . Middelburg, J. J. (2007). Plumbing the global carbon cycle: integrating inland waters into the terrestrial carbon budget. Ecosystems, 10(1), 172-185.

Correa-González, J. C., del Carmen Chávez-Parga, M., Cortés, J. A., & Pérez-Munguía, R. M. (2014). Photosynthesis, respiration and reaeration in a stream with complex dissolved oxygen pattern and temperature dependence. Ecological modelling, 273, 220-227.

Dodds, W. K., Biggs, B. J. F., & Lowe, R. L. (1999). Photosynthesis - irradiance patterns in benthic microalgae: variations as a function of assemblage thickness and community structure. Journal of Phycology, 35(1), 42-53.

Dodds, W. K., Higgs, S. A., Spangler, M. J., Guinnip, J., Scott, J. D., Hedden, S. C., . . . Hoeinghaus, D. J. (2018). Spatial heterogeneity and controls of ecosystem metabolism in a Great Plains river network. Hydrobiologia, 813(1), 85-102.

Cooper, S. D., Lake, P. S., Sabater, S., Melack, J. M., & Sabo, J. L. (2013). The effects of land use changes on streams and rivers in mediterranean climates. Hydrobiologia, 719(1), 383-425.

Duff, J. H., Tesoriero, A. J., Richardson, W. B., Strauss, E. A., & Munn, M. (2008). Whole-stream response to nitrate loading in three streams draining agricultural landscapes. USGS Staff--Published Research, 25.

Fellows, C. S., Clapcott, J. E., Udy, J. W., Bunn, S. E., Harch, B. D., Smith, M. J., & Davies, P. M. (2006). Benthic metabolism as an indicator of stream ecosystem health. Hydrobiologia, 572(1), 71-87.

Finlay, J. C. (2011). Stream size and human influences on ecosystem production in river networks. Ecosphere, 2(8), 1-21.

Finlay, L. (2011). Phenomenology for therapists: Researching the lived world: John Wiley & Sons.

Fisher, S. G., Gray, L. J., Grimm, N. B., & Busch, D. E. (1982). Temporal succession in a desert stream ecosystem following flash flooding. Ecological Monographs, 52(1), 93-110.

Foufoula-Georgiou, E., & Kumar, P. (2014). Wavelets in geophysics: Elsevier.

Gleick, P. H. (2003). Water use. Annual review of environment and resources, 28(1), 275-314.

Griffiths, N. A., Tank, J. L., Royer, T. V., Roley, S. S., Rosi-Marshall, E. J., Whiles, M. R., . . . Johnson, L. T. (2013). Agricultural land use alters the seasonality and magnitude of stream metabolism. Limnology and Oceanography, 58(4), 1513-1529. doi:10.4319/lo.2013.58.4.1513

Grimm, N. B. (1987). Nitrogen dynamics during succession in a desert stream. Ecology, 68(5), 1157-1170.

Grimm, N. B., & Fisher, S. G. (1984). Exchange between interstitial and surface water: implications for stream metabolism and nutrient cycling. Hydrobiologia, 111(3), 219-228.

Grimm, N. B., & Fisher, S. G. (1986). Nitrogen limitation in a Sonoran Desert stream. Journal of the North American Benthological Society, 5(1), 2-15.

Grimm, N. B., & Fisher, S. G. (1989). Stability of periphyton and macroinvertebrates to disturbance by flash floods in a desert stream. Journal of the North American Benthological Society, 8(4), 293-307.

Grimm, N. B., Sheibley, R. W., Crenshaw, C. L., Dahm, C. N., Roach, W. J., & Zeglin, L. H. (2005). N retention and transformation in urban streams. Journal of the North American Benthological Society, 24(3), 626-642.

Guasch, H., Martí, E., & Sabater, S. (1995). Nutrient enrichment effects on biofilm metabolism in a Mediterranean stream. Freshwater biology, 33(3), 373-383.

Gücker, B., & Pusch, M. T. (2006). Regulation of nutrient uptake in eutrophic lowland streams. Limnology and Oceanography, 51(3), 1443-1453.

Guecker, B., Boechat, I. G., & Giani, A. (2009). Impacts of agricultural land use on ecosystem structure and whole ‐ stream metabolism of tropical Cerrado streams. Freshwater biology, 54(10), 2069-2085.

Guecker, B., Boëchat, I. G., & Giani, A. (2009). Impacts of agricultural land use on ecosystem structure and whole-stream metabolism of tropical Cerrado streams. Freshwater biology, 54(10), 2069-2085. doi:10.1111/j.1365-2427.2008.02069.x

Hall Jr, R. O. (2016). Metabolism of streams and rivers: Estimation, controls, and application. In Stream ecosystems in a changing environment (pp. 151-180): Elsevier.

Hall, R. J. O., & Tank, J. L. (2003). Ecosystem metabolism controls nitrogen uptake in streams in Grand Teton National Park, Wyoming. Limnology and Oceanography, 48(3), 1120-1128.

Hall, R. O., & Beaulieu, J. J. (2013). Estimating autotrophic respiration in streams using daily metabolism data. Freshwater Science, 32(2), 507-516. doi:10.1899/12-147.1

Hamada, Y., O'Connor, B. L., Orr, A. B., & Wuthrich, K. K. (2016). Mapping ephemeral stream networks in desert environments using very-high-spatial-resolution multispectral remote sensing. Journal of Arid Environments, 130, 40-48.

Hoellein, T. J., Bruesewitz, D. A., & Richardson, D. C. (2013). Revisiting Odum (1956): A synthesis of aquatic ecosystem metabolism. Limnology and Oceanography, 58(6), 2089-2100.

Hondzo, M., Voller, V. R., Morris, M., Foufoula‐Georgiou, E., Finlay, J., Ganti, V., & Power, M. E. (2013). Estimating and scaling stream ecosystem metabolism along channels with heterogeneous substrate. Ecohydrology, 6(4), 679-688.

Howarth, R. W., Fruci, J. R., & Sherman, D. (1991). Inputs of sediment and carbon to an estuarine ecosystem: influence of land use. Ecological Applications, 1(1), 27-39.

Izagirre, O., Agirre, U., Bermejo, M., Pozo, J., & Elosegi, A. (2008). Environmental controls of whole-stream metabolism identified from continuous monitoring of Basque streams. Journal of the North American Benthological Society, 27(2), 252-268.

Jones Jr, J. (1995). Factors controlling hyporheic respiration in a desert stream. Freshwater biology, 34(1), 91-99.

Jones Jr, J. B., Fisher, S. G., & Grimm, N. B. (1995). Nitrification in the hyporheic zone of a desert stream ecosystem. Journal of the North American Benthological Society, 14(2), 249-258.

Koenig, L. E., Helton, A. M., Savoy, P., Bertuzzo, E., Heffernan, J. B., Hall Jr, R. O., & Bernhardt, E. S. (2019). Emergent productivity regimes of river networks. Limnology and Oceanography Letters, 4(5), 173-181.

Koenig, P., Mangler, J., & Rinderle-Ma, S. (2019). Compliance monitoring on process event streams from multiple sources.

Lake, P. S. (2003). Ecological effects of perturbation by drought in flowing waters. Freshwater biology, 48(7), 1161-1172.

Lamberti, G. A., & Steinman, A. D. (1997). A comparison of primary production in stream ecosystems. Journal of the North American Benthological Society, 16(1), 95-104.

Larned, S. T., Datry, T., Arscott, D. B., & Tockner, K. (2010). Emerging concepts in temporary‐river ecology. Freshwater biology, 55(4), 717-738.

Leggieri, L., Feijoó, C., Giorgi, A., Ferreiro, N., & Acuña, V. (2013). Seasonal weather effects on hydrology drive the metabolism of non-forest lowland streams. Hydrobiologia, 716(1), 47-58.

Marzolf, E. R., Mulholland, P. J., & Steinman, A. D. (1994). Improvements to the diurnal upstream–downstream dissolved oxygen change technique for determining whole-stream metabolism in small streams. Canadian Journal of Fisheries and Aquatic Sciences, 51(7), 1591-1599.

Marzolf, N. S., & Ardón, M. (2021). Ecosystem metabolism in tropical streams and rivers: a review and synthesis. Limnology and Oceanography, 66(5), 1627-1638.

Merseburger, G., Martí, E., Sabater, F., & Ortiz, J. D. (2011). Point-source effects on N and P uptake in a forested and an agricultural Mediterranean streams. Science of the total environment, 409(5), 957-967.

Meyer, A., Meyer, E. I., & Meyer, C. (2003). Lotic communities of two small temporary karstic stream systems (East Westphalia, Germany) along a longitudinal gradient of hydrological intermittency. Limnologica, 33(4), 271-279.

Minshall, G. W. (1978). Autotrophy in stream ecosystems. BioScience, 28(12), 767-771.

Moran, N. P., Wong, B. B., & Thompson, R. M. (2019). Communities at the extreme: Aquatic food webs in desert landscapes. Ecology and evolution, 9(19), 11464-11475.

Moran, N. P., Wong, B. B. M., & Thompson, R. M. (2019). Communities at the extreme: Aquatic food webs in desert landscapes. Ecology and evolution, 9(19), 11464-11475.

Mulholland, M. R., Ohki, K., & Capone, D. G. (2001). Nutrient controls on nitrogen uptake and metabolism by natural populations and cultures of Trichodesmium (Cyanobacteria). Journal of Phycology, 37(6), 1001-1009.

Mulholland, P., Fellows, C., Tank, J., Grimm, N., Webster, J., Hamilton, S., . . . Dodds, W. (2001). Inter‐biome comparison of factors controlling stream metabolism. Freshwater biology, 46(11), 1503-1517.

Mulholland, P. J., Fellows, C. S., Tank, J. L., Grimm, N. B., Webster, J. R., Hamilton, S. K., . . . Dodds, W. K. (2001). Inter‐biome comparison of factors controlling stream metabolism. Freshwater biology, 46(11), 1503-1517.

Mulholland, P. J., Helton, A. M., Poole, G. C., Hall, R. O., Hamilton, S. K., Peterson, B. J., . . . Dahm, C. N. (2008). Stream denitrification across biomes and its response to anthropogenic nitrate loading. Nature, 452(7184), 202-205.

Mulholland, P. J., Tank, J. L., Sanzone, D. M., Wollheim, W. M., Peterson, B. J., Webster, J. R., & Meyer, J. L. (2000). Nitrogen cycling in a forest stream determined by a 15N tracer addition. Ecological Monographs, 70(3), 471-493.

Nadeau, T. L., & Rains, M. C. (2007). Hydrological connectivity between headwater streams and downstream waters: how science can inform policy 1. JAWRA Journal of the American Water Resources Association, 43(1), 118-133.

Naiman, R. J. (1983). The annual pattern and spatial distribution of aquatic oxygen metabolism in boreal forest watersheds. Ecological Monographs, 53(1), 73-94.

O'Connor, B. L., Harvey, J. W., & McPhillips, L. E. (2012). Thresholds of flow‐induced bed disturbances and their effects on stream metabolism in an agricultural river. Water Resources Research, 48(8).

Odum, H. T. (1956). Primary production in flowing waters. Limnology and Oceanography, 1(2), 102-117.

Odum, H. T. (1956). Primary production in flowing waters 1. Limnology and Oceanography, 1(2), 102-117.

Perkins, S. E., Alexander, L. V., & Nairn, J. R. (2012). Increasing frequency, intensity and duration of observed global heatwaves and warm spells. Geophysical Research Letters, 39(20).

Peterson, J. M., & Boisvert, R. N. (2001). Control of nonpoint source pollution through voluntary incentive-based policies: an application to nitrate contamination in New York. Agricultural and Resource Economics Review, 30(2), 127-138.

Post, D. M., Doyle, M. W., Sabo, J. L., & Finlay, J. C. (2007). The problem of boundaries in defining ecosystems: a potential landmine for uniting geomorphology and ecology. Geomorphology, 89(1-2), 111-126.

Power, M. E., & Stewart, A. J. (1987). Disturbance and recovery of an algal assemblage following flooding in an Oklahoma stream. American Midland Naturalist, 333-345.

Roberts, J. H., & Angermeier, P. L. (2007). Spatiotemporal variability of stream habitat and movement of three species of fish. Oecologia, 151(3), 417-430.

Roesch, A., Schmidbauer, H., & Roesch, M. A. (2014). Package 'WaveletComp'. The Comprehensive R Archive Network2014.

Sabo, J. L., & Post, D. M. (2008). Quantifying periodic, stochastic, and catastrophic environmental variation. Ecological Monographs, 78(1), 19-40.

Sabo, J. L., Ruhi, A., Holtgrieve, G. W., Elliott, V., Arias, M. E., Ngor, P. B., . . . Nam, S. (2017). Designing river flows to improve food security futures in the Lower Mekong Basin. Science, 358(6368).

Sabo, J. L., Sinha, T., Bowling, L. C., Schoups, G. H. W., Wallender, W. W., Campana, M. E., . . . Hopmans, J. W. (2010). Reclaiming freshwater sustainability in the Cadillac Desert. Proceedings of the National Academy of Sciences, 107(50), 21263-21269.

Savoy, P., Appling, A. P., Heffernan, J. B., Stets, E. G., Read, J. S., Harvey, J. W., & Bernhardt, E. S. (2019). Metabolic rhythms in flowing waters: An approach for classifying river productivity regimes. Limnology and Oceanography, 64(5), 1835-1851.

Shah, S., Sharma, M., Deb, D., & Pachori, R. B. (2019). An automated alcoholism detection using orthogonal wavelet filter bank. In Machine Intelligence and Signal Analysis (pp. 473-483): Springer.

Sinsabaugh, R. L., Carreiro, M. M., & Repert, D. A. (2002). Allocation of extracellular enzymatic activity in relation to litter composition, N deposition, and mass loss. Biogeochemistry, 60(1), 1-24.

Sinsabaugh, R. L., Findlay, S., Franchini, P., & Fischer, D. (1997). Enzymatic analysis of riverine bacterioplankton production. Limnology and Oceanography, 42(1), 29-38.

Sobota, D. J., Johnson, S. L., Gregory, S. V., & Ashkenas, L. R. (2012). A stable isotope tracer study of the influences of adjacent land use and riparian condition on fates of nitrate in streams. Ecosystems, 15(1), 1-17.

Tank, J. L., Rosi-Marshall, E. J., Griffiths, N. A., Entrekin, S. A., & Stephen, M. L. (2010). A review of allochthonous organic matter dynamics and metabolism in streams. Journal of the North American Benthological Society, 29(1), 118-146.

Torrence, C., & Compo, G. P. (1998). A practical guide to wavelet analysis. Bulletin of the American Meteorological society, 79(1), 61-78.

Tranvik, L. J., Downing, J. A., Cotner, J. B., Loiselle, S. A., Striegl, R. G., Ballatore, T. J., . . . Knoll, L. B. (2009). Lakes and reservoirs as regulators of carbon cycling and climate. Limnology and Oceanography, 54(6part2), 2298-2314.

Uehlinger, U. (2006). Annual cycle and inter ‐ annual variability of gross primary production and ecosystem respiration in a floodprone river during a 15 ‐ year period. Freshwater biology, 51(5), 938-950.

Uehlinger, U., Naegeli, M., & Fisher, S. G. (2002). A heterotrophic desert stream? The role of sediment stability. Western North American Naturalist, 466-473.

Uehlinger, U., & Naegeli, M. W. (1998). Ecosystem metabolism, disturbance, and stability in a prealpine gravel bed river. Journal of the North American Benthological Society, 17(2), 165-178.

Uehlinger, U. R. S. (2006). Annual cycle and inter-annual variability of gross primary production and ecosystem respiration in a floodprone river during a 15-year period. Freshwater biology, 51(5), 938-950. doi:10.1111/j.1365-2427.2006.01551.x

Ulseth, A. J., Hall, R. O., Canadell, M. B., Madinger, H. L., Niayifar, A., & Battin, T. J. (2019). Distinct air–water gas exchange regimes in low-and high-energy streams. Nature Geoscience, 12(4), 259-263.

Vilches, C., & Giorgi, A. (2010). Metabolism in a macrophyte-rich stream exposed to flooding. Hydrobiologia, 654(1), 57-65.

Webster, J. R., & Meyer, J. L. (1997). Organic matter budgets for streams: a synthesis. Journal of the North American Benthological Society, 16(1), 141-161.

Webster, J. R., Wallace, J. B., & Benfield, E. F. (1995). Organic processes in streams of the eastern United States. River stream Ecosyst. world, 117-187.

Williamson, C. E., Dodds, W., Kratz, T. K., & Palmer, M. A. (2008). Lakes and streams as sentinels of environmental change in terrestrial and atmospheric processes. Frontiers in Ecology and the Environment, 6(5), 247-254.

Yates, A. G., Brua, R. B., Culp, J. M., & Chambers, P. A. (2013). Multi-scaled drivers of rural prairie stream metabolism along human activity gradients. Freshwater biology, 58(4), 675-689. doi:10.1111/fwb.12072

Yates, A. G., Brua, R. B., Culp, J. M., & Chambers, P. A. (2013). Multi‐scaled drivers of rural prairie stream metabolism along human activity gradients. Freshwater biology, 58(4), 675-689.

Young, R. G., & Huryn, A. D. (1999). Effects of land use on stream metabolism and organic matter turnover. Ecological Applications, 9(4), 1359-1376.

Zuur, A. F., Ieno, E. N., Walker, N. J., Saveliev, A. A., & Smith, G. M. (2009). Mixed effects models and extensions in ecology with R (Vol. 574): Springer.

APPENDIX A

TABLES & FIGURES

TABLE S1: THE PERCENTAGE OF TIMING OF THE ANNUAL EXTREME RESIDUALS OCCURRED IN EACH QUARTER OF THE YEAR, 2000-2020. Annual.max and annial.min were referred as the most extreme high-flow and low-flow events annually. For example, in AF (Agua Fria River), 38.10% of the most extreme high-flow events occurred in the 1st quarter of the year in the most recent 20 years' record.

type	site	1st quarter	2nd quarter	3rd quarter	4th quarter
annual.max	AF	38.10%	0	38.10%	23.80%
	BB	14.30%	4.80%	71.40%	9.50%
	BN	28.60%	14.30%	52.40%	4.80%
	EG	38.10%	4.80%	52.40%	4.80%
	RM	28.60%	4.80%	52.40%	14.30%
	SC	9.50%	4.80%	76.20%	9.50%
	SF	28.60%	0	38.10%	33.30%
	SP	4.80%	4.80%	76.20%	14.30%
	SY	52.40%	0	28.60%	19.00%
	VD	33.30%	4.80%	57.10%	4.80%
	WB	47.60%	0	23.80%	28.60%
annual.min	AF	19.00%	0	81.00%	0
	BB	4.80%	0	61.90%	33.30%
	BN	47.60%	0	28.60%	23.80%
	EG	52.40%	4.80%	38.10%	4.80%
	RM	28.60%	4.80%	61.90%	4.80%
	SC	4.80%	0	95.20%	0
	SF	4.80%	42.90%	47.60%	4.80%
	SP	4.80%	0	95.20%	0
	SY	66.70%	9.50%	9.50%	14.30%
	VD	95.20%	4.80%	0	0
	WB	81.00%	19.00%	0	0

FIGURE S1: DFFT RESULT FOR ALL 11 STREAMS. a- k: Annual extreme residuals of discharge along time (X axis: year; Y axis: Residual event magnitude; dash line: low-flow event magnitude equal to 2 sigma; dotted line: high-flow event magnitude equal to 2 sigma; empty square: annual extreme high-flow residuals; empty dot: annual extreme low-flow residuals. A- K: Net annual anomalies (upper, red: dry regime with negative NAA; blue: wet regime with positive NAA) and delta net annual anomalies of each year (lower, red: dry regime without regime shift; green: regime shift from dry to wet; blue: regime shift from wet to dry; purple: wet regime without regime shift).

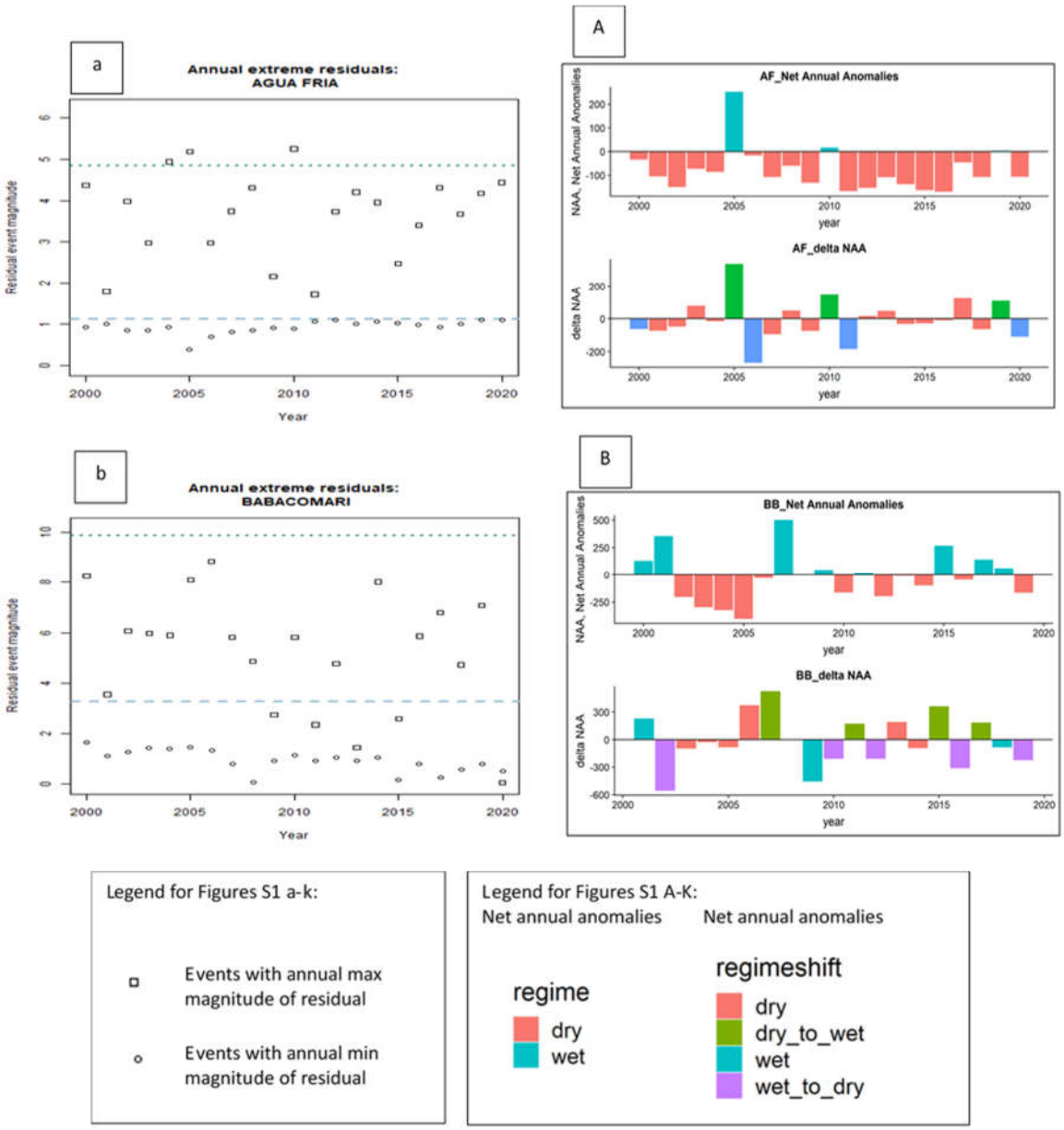

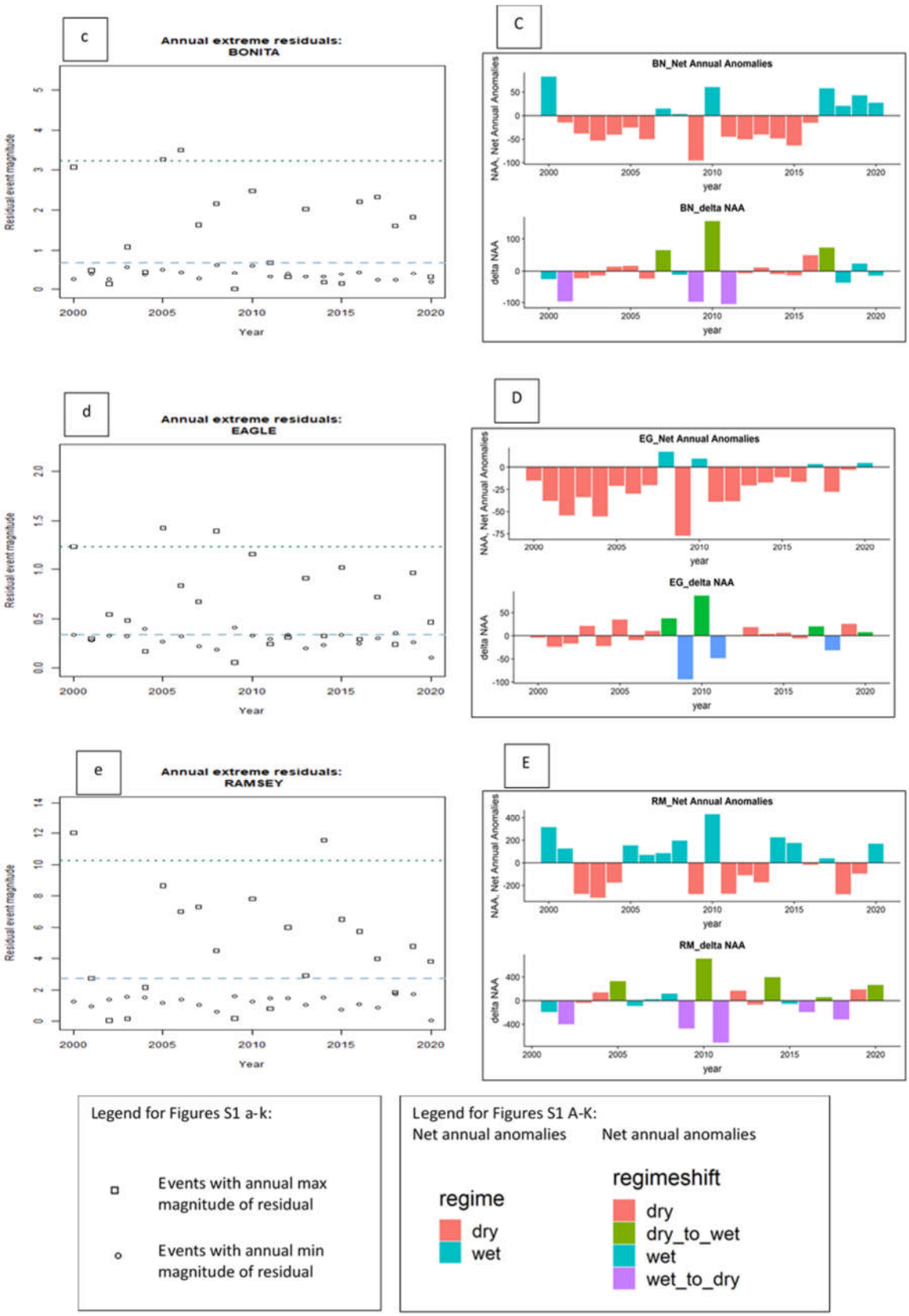
c
Annual extreme residuals:
BONITA
Residual event magnitude
Year
C
BN_Net Annual Anomalies
NAA, Net Annual Anomalies
year
BN_delta NAA
delta NAA
year
d
Annual extreme residuals:
EAGLE
Residual event magnitude
Year
D
EG_Net Annual Anomalies
NAA, Net Annual Anomalies
year
EG_delta NAA
delta NAA
year
e
Annual extreme residuals:
RAMSEY
Residual event magnitude
Year
E
RM_Net Annual Anomalies
NAA, Net Annual Anomalies
year
RM_delta NAA
delta NAA
year
Legend for Figures S1 a-k:
Events with annual max magnitude of residual
Events with annual min magnitude of residual
Legend for Figures S1 A-K:
Net annual anomalies
Net annual anomalies
regime
dry
wet
regimeshift
dry
dry_to_wet
wet
wet_to_dry

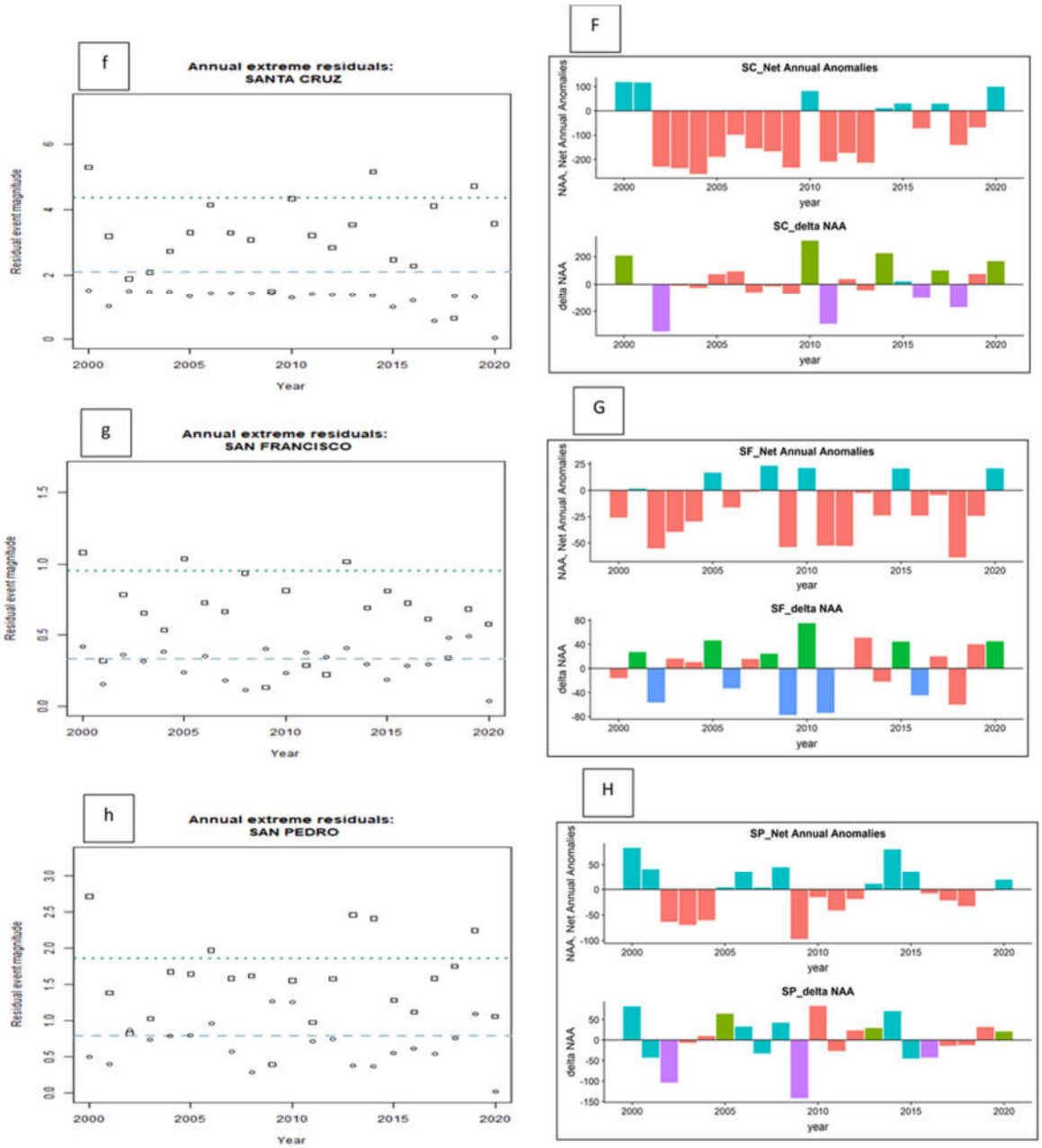

Legend for Figures S1 a-k:

□ Events with annual max magnitude of residual

○ Events with annual min magnitude of residual

Legend for Figures S1 A-K:

Net annual anomalies

regime
- dry
- wet

Net annual anomalies

regimeshift
- dry
- dry_to_wet
- wet
- wet_to_dry

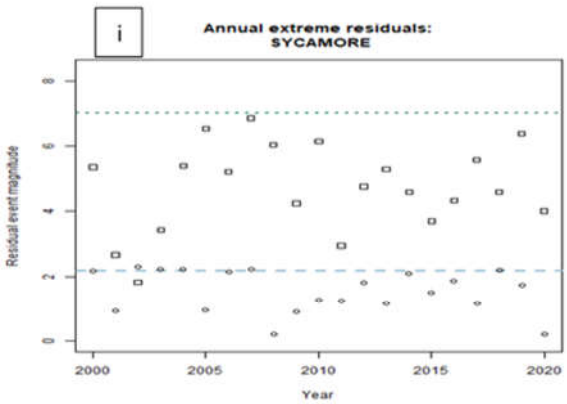

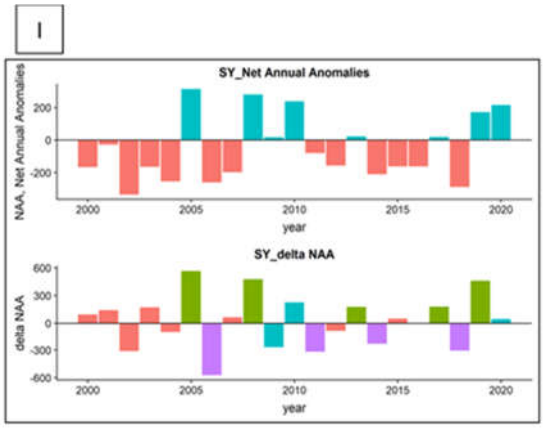

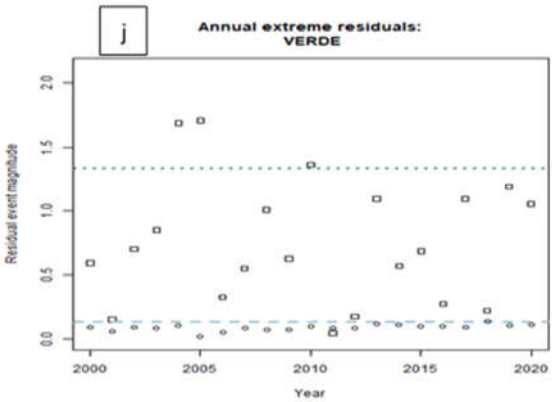

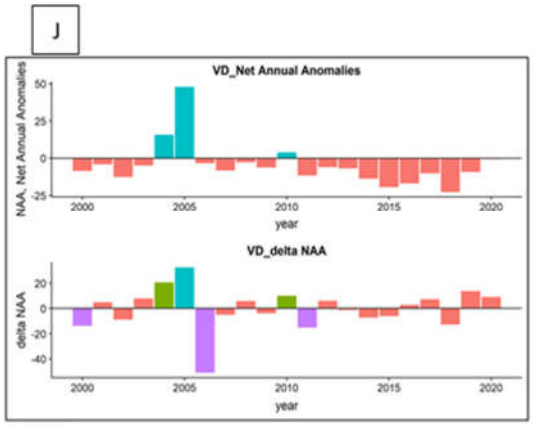

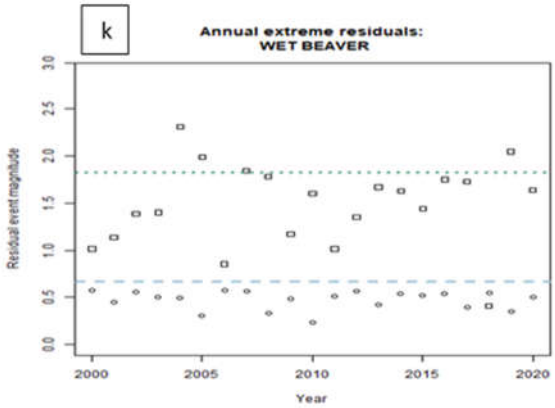

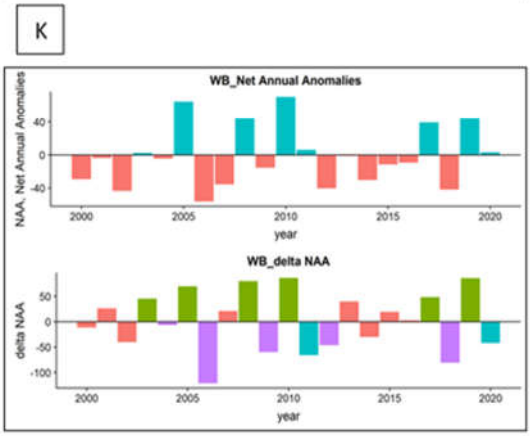

Legend for Figures S1 a-k:

□ Events with annual max magnitude of residual

○ Events with annual min magnitude of residual

Legend for Figures S1 A-K:

Net annual anomalies

regime
- dry
- wet

Net annual anomalies

regimeshift
- dry
- dry_to_wet
- wet
- wet_to_dry

FIGURE S2: SCALE-AVERAGE TIME SERIES OF MAX ANNUAL AGGREGATE BLUE NOISE POWER ALONG TIME FOR ALL 11 STREAMS. X axis: year, Y: aggregate blue noise power.

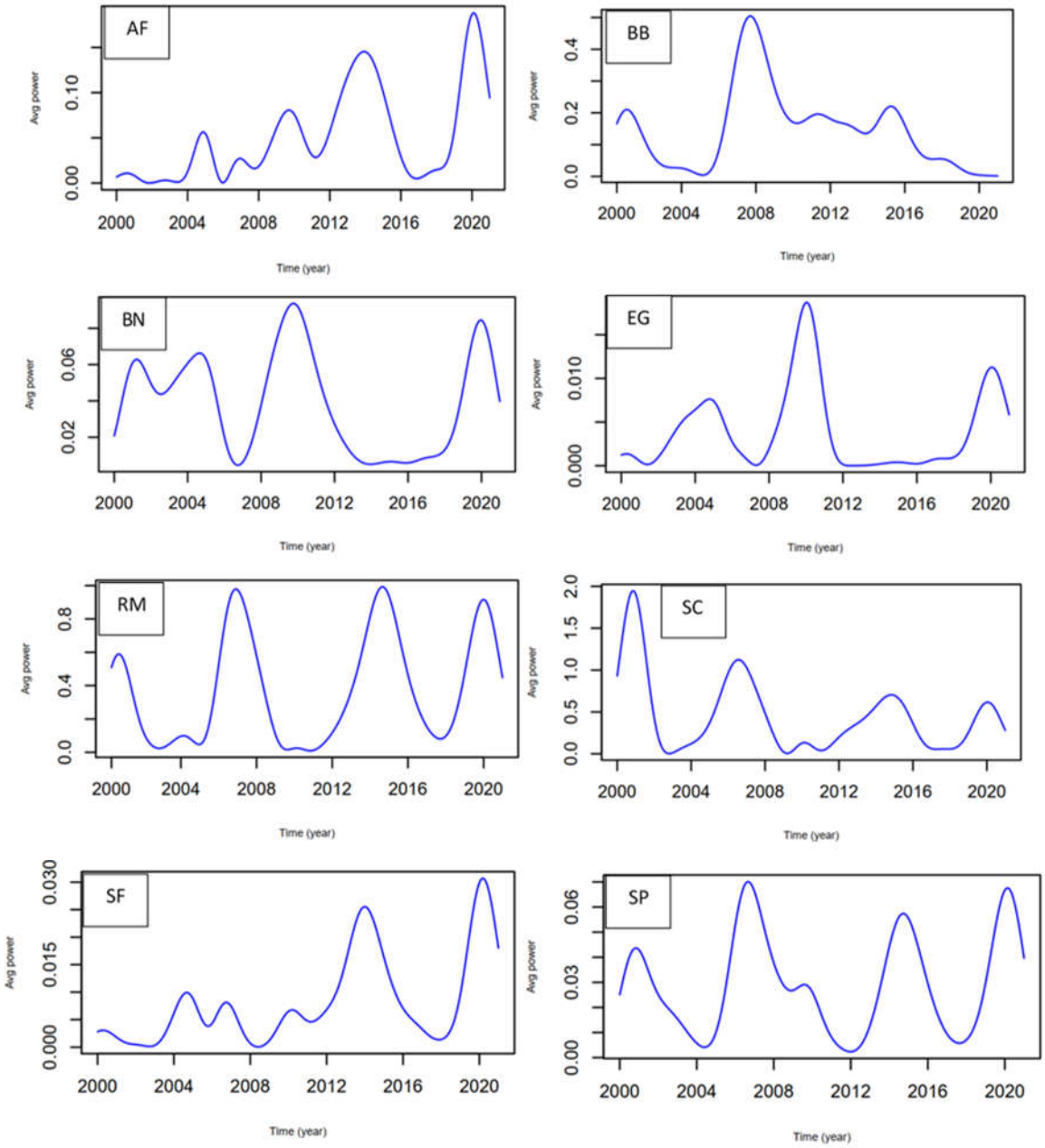

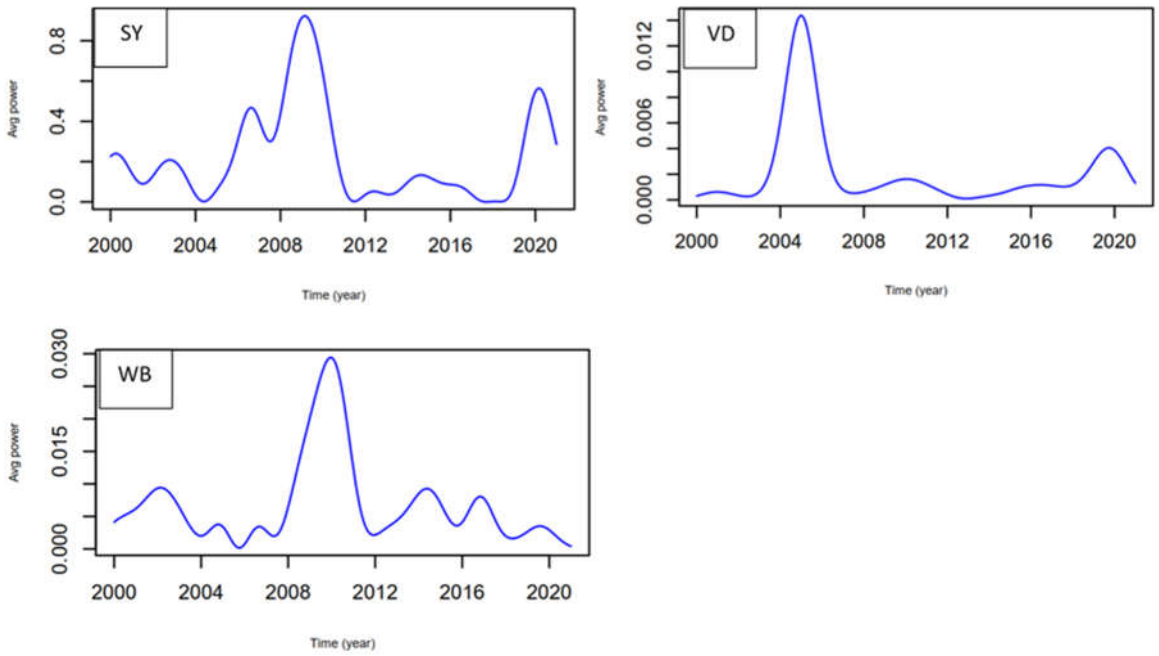
SY
Avg power
0.0
0.4
0.8
2000
2004
2008
2012
2016
2020
Time (year)
VD
Avg power
0.000
0.006
0.012
2000
2004
2008
2012
2016
2020
Time (year)
WB
Avg power
0.000
0.015
0.030
2000
2004
2008
2012
2016
2020
Time (year)